2D SEISMIC REFLECTION DATA INTERPRETATION INTEGRATED WITH RESERVOIR CHARACTERIZATION OF MIANO AREA USING SEISMIC AND WELL LOG DATA

BY

Zubair Abdullah

BS. Geophysics

2013-2017

Department of Earth Sciences

Quaid-i-Azam University Islamabad

I commence with the Name of Allah - in whom all excellences are Combined and who is free from all defects. The Compassionate One whose blessings are extensive and unlimited. The Merciful One whose blessings are inherent and eternal.

CERTIFICATE

This dissertation submitted by **Zubair Abdullah** S/O **Abdul Manan Khalid** is accepted in its present form by the Department of Earth Sciences, Quaid-I-Azam University Islamabad as satisfying the requirement for the award of BS. Degree in Geophysics

RECOMMENDED BY

Dr. Aamir Ali _____

(Supervisor)

Prof Dr. Mona Lisa _____

(Chairperson Department of Earth Sciences)

EXTERNAL EXAMINER _____

Department of Earth Sciences Quaid-i-Azam University Islamabad, Pakistan

Summary

Reservoir characterization using seismic and well data is a renowned technique within the content of hydrocarbon exploration. This study pertains to the interpretation of seismic lines, wireline logs and amplitude versus offset (AVO) modeling for improved characterization of reservoir level in Miano area, Lower Indus Basin, Pakistan.

Geologically Miano area is found at the boundary of Central and Southern Indus Basin. This thesis work includes preparation of synthetic seismogram of Miano-09 well. Analysis of geophysical borehole logs provides one of the best approaches to characterizing rocks within boreholes.

For the interpretation of the seismic lines, fours reflectors are marked by correlating synthetic seismogram on seismic section. As the area of study lies in the Lower Indus Basin, horst and graben geometry in this region is common which is confirmed by fault polygon and time and depth contours made from time and depth grid respectively.

Petrophysics is the one of the most reliable tools for the confirmation of the types of the hydrocarbon and for marking of the proper zone of the interest of the presence of the hydrocarbon by combination of the different logs results. In this dissertation the petrophysics is performed on the Miano-09 well and zone of interest is marked at depth of 3331-3385m, which is the B-interval of Lower Goru sand formation. This zone contain 51.7% of water saturation and 47.2% of hydrocarbon saturation. At last the AVO modeling is performed in order to identify the class of the sand present in the reservoir zone. From AVO modeling it is confirmed that the B-interval sand of Lower Goru formation is class one sand.

ACKNOWLEDGEMENT

First praise is to Allah, the most Beneficent, Merciful and Almighty, on whom ultimately we depend for sustenance and guidance. I bear witness that Holy Prophet Muhammad (PBUH) is the last messenger, whose life is perfect model for the whole mankind till the Day of Judgment. I thank Allah for giving me strength and ability to complete this study.

I am especially indebted to my honorable supervisor DR. Aamir Ali for giving me an initiative to this study. His inspiring guidance, dynamic supervision and constructive criticism, helped me to complete this work in time.

I specially acknowledge the prayers and efforts of my whole family, specially my parents my brother for their encouragement, support and sacrifices throughout the study. I also wish to thank the whole faculty of my department for providing me with an academic base, which has enabled me to take up this study I pay my thanks to the employees of clerical office who helped me a lot and all those their names do not appear here who have contributed to the successful completion of this study. I would like to thanks who helps me in studies whenever I needed.

My friends and my thesis mates Usman Nadeem Faroqui, Aqeel Abbas Magsi and Muhammad Usman who encouraged me with constant motivation and my parent's encouragement played a role of back bone throughout my academic carrier.

Zubair Abdullah

BS. Geophysics (2013-2017)

Table of Contents

List of Figures

List of Table

Chapter 1

Introduction

1.1 Introduction

Hydrocarbon is major source of energy, it play a key role in economy of the every country. Geophysical method are widely used in exploration of hydrocarbon. Seismic method is an important method for exploration (Kearey et al., 2013). In seismic method acoustic wave is emitted from a source and send into the earth. This wave is bounced back after hitting from different geological boundary in the subsurface and reached at the sensor. It give the detail information about the earth model and distance of the earth layers from the source (Onajite, 2013). Seismic reflection method has greater precision than refraction method for deep hydrocarbon exploration in petroleum geology. It defines the set of disciplines which are used for hydrocarbon. Oil and gas fields are results from the geological features which are source rocks, Migration, reservoir rocks, seals, and traps (Sroor, 2010). So the knowledge about geology of area is important for exploration point of view. The aim of study is to map the subsurface geology. For this purpose different Geophysical techniques are used to analyze the seismic data for characterization of reservoir. To serve this purpose, 2D seismic data which is in SEG-Y format and well logs information are used. After interpretation of seismic profile these profiles are transformed into 2D and 3D (Time and Depth domain) contour maps, which represents the true subsurface geology (Khan et al., 2016).

Petrophysics help us for characterization and understanding of our reservoir by knowing the rock and fluid properties such as permeability, fluid saturations, porosity, lithology and rock mechanical properties. The results of these parameters help us to determine reservoir predictability and devise long-term field development strategies. Petrophysics in petroleum industry is used for the characterization and determination of the rock and fluid properties of reservoir and non-reservoir strata (Steve, 2015).

- It determine the nature of interconnected network of pore space-**porosity.**
- The distribution of oil, water and gas in pore spaces-**water saturation**.
- The potential for the fluid to flow through the network-**permeability.**

Seismic attributes have become an most important and power tool for interpretation since 1970. This consider as management display tool. There are numbers of attributes which are amplitude, velocity, rate of change of them with respect to time or space. We can compute some of attributes by complex trace which are envalop, phase etc. corresponding to the measurement of the propagating wave-front (Taner et al., 1994).

Seismic attributes are the components of the seismic data, which are obtained by measurement computation, and other method from the seismic data. Seismic attribute use information from seismic data which is hidden in data to determine prospects, ascertain depositional environments

(Koson et al., 2014). Seismic attributes give information about seismic interpretation and is useful tool for conformation of horizon and fault picking and to recognize the deposition setting of the strata.

Amplitude variation with offset (AVO) is a technique used in petroleum industry for detection of hydrocarbon (Rutherford and Williams, 1989). It is a tool which is used to differentiate the reflection events due to change in lithology and also change due to fluid is known as amplitude versus offset (Crain, 2013). We can derive the rock properties with the help of amplitude variation with offset (AVO). When a seismic wave hit the boundary at the interface at an angle a part of energy is transmitted and the other part is reflected from the interface. Reflection amplitude rely on the angle of incidence of wave (Michael Burianyk, 2000). Two factors which are helpful for the determination of gas sand reflections are Poisson's ratio and normal incidence reflection coefficient at the reflector (Rutherford and Williams, 1989).

1.2 Objectives

The main objective of dissertation is determination of reservoir zone in the study area and to see the subsurface structure in the study area by marking the fault at the discontinuity of the strata. It can be seen on seismic section by horizons and faults.

- Detailed 2D seismic data interpretation of the area for identification of the subsurface structural trends which are favorable for accumulation of hydrocarbons.
- Petrophysical analysis of Miano-09 well for identification of favorable zone for hydrocarbon accumulation and their reservoir characteristics.
- Seismic attributes analysis to confirm interpretation.
- AVO modelling for determination of different classes of sand at the well point.

1.3 Data used

In 1994 2-D seismic data is acquired in the half of the block-20 Miano area. 2-D seismic reflection data and les file of Miano-09 well is provided by institute. Table 1.1 shows the detail of seismic data used in dissertation. It shows line P2094-219 and P2094-223 are dip lines with orientation E-W whereas P2094-214 are strike line with orientation N-S. Dip lines shows the regional geologic subsurface structure and these lines are small while strike lines are large and did not shows the subsurface structures regionally because these lines are along the fault.

Sr.no	Line name	Orientation	Nature	Sp range
1	P2094-219	E-W	Dip	102-1140
2	P2094-223	E-W	Dip	102-1153
3	P2094-214	N-S	Strike	102-1175

Table 1.1 Lines of area which are used in dissertation.

Only one well is used which is Miano-09 well. Table 1.2 shows the latitude, longitude and elevation of well.

Well name	Longitude	Latitude	Total elevation	Status
Miano-09	69.3111487	27.371747	3385	Exploration gas

Table 1.2 Information of well which is used in dissertation.

1.4 Location of study area

Miano (Block-20) area is located in Sindh province and tectonically it is lies in lower Indus basin (Rehman et al., 2013). This field lies in the Thar Desert 62km southeast of Sukkur, Pakistan (khan et al., 2017). The field is approximately 42km long along the strike. The southernmost well in the field is about 10 kilometers away from Kadanwari field and 45 kilometers from the Sawan Gas field to the southwest. Mari gas and Sui gas are the two largest fields which are producing from the Eocene aged Sui main limestone. These fields are located 75km and 150km to the north of the study area. Figure 1.1 shows the tectonic map of Pakistan which highlights that Miano area tectonically lies in which zone. Cretaceous extensional faults which are trending NNW to SSE direction are mostly found in Miano area. The Lower Goru sand of Lower Cretaceous age are acting as a reservoir in the area. Geologically it is bounded between the Indian basements, the Kirther f old and thrust belt. Survey was carried out by OMV in 1994. The purpose of study is to locate the prospective zone. The Geographic coordinates of the area are 27° 14' N to 27° 32' N and 69° 12' E to 69° 28' E.

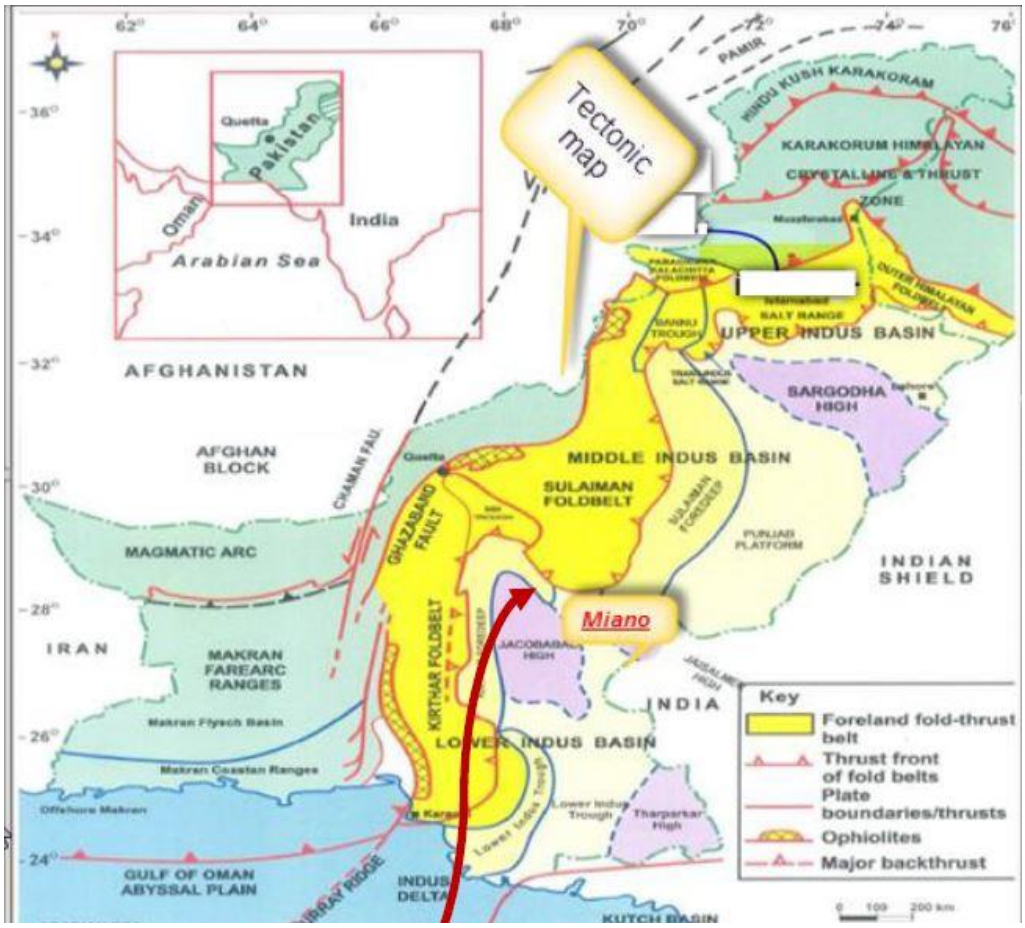

Figure 1.1 Geographical location of Miano area (Nadeem et al., 2004).

1.1 Brief overview of the thesis

For completion of objectives the dissertation work is divided into 5 chapters. 1st chapter include general introduction, 2nd chapter include general geology and stratigraphy of the area. In 3rd chapter there is complete seismic interpretation of the area by using kingdom software. Then in 4th chapter we do petrophysics by using kingdom software to find the different portion of hydrocarbon and water in the reservoir zone. Then in the last chapter we do AVO modelling to identify the class of sand by using Matlab software. Figure 1.2 shows the procedure of the work first we load the data on kingdom software then to make a basemap, then generate synthetic seismogram to confirm the formation. Then in next step we mark the horizons and faults then we make fault polygons and then we make a grid over it and contour it. We apply seismic attribute on seismic section to see that horizon and faults are marked correctly or not. Then we do petrophysics to mark the probable zone then finaly we do AVO modelling to see the class of sand.

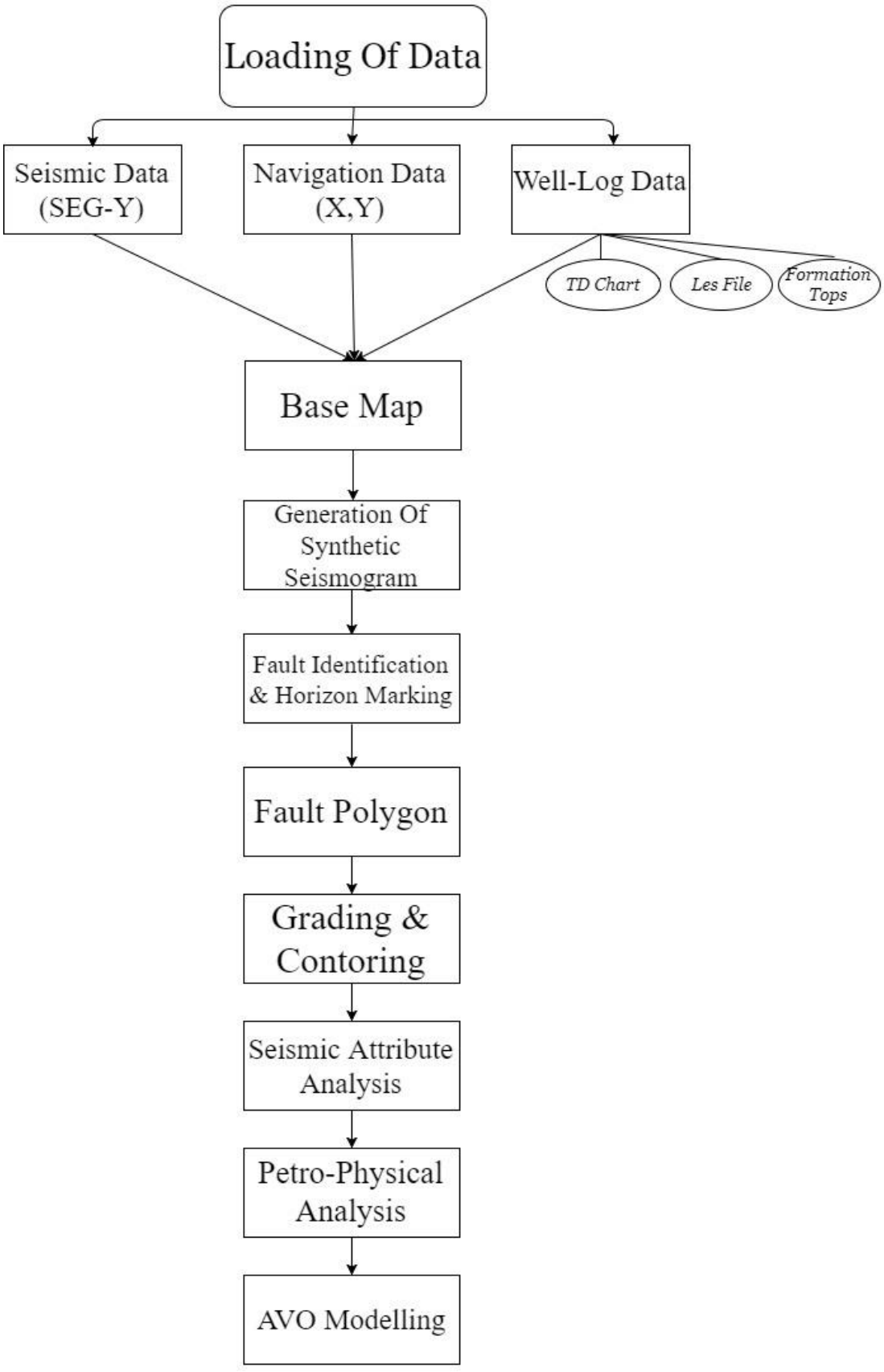

Figure 1.2 Work Flow of Dissertation.

Chapter 2

General geology

2.1 Introduction

For exploration of oil or gas, the knowledge about the history and geology of the area is most important. In Cretaceous period west Gondwana plate (Africa and South America) separated from East Gondwana plate (India, Antarctica and Australia). Indian plate separated from east Gondwana plate in Aptian time (Gibbons et al., 2013).

Powell (1979) The Tectonic history of Pakistan and surroundings are defined in an article that india is separated from Seychelles and Madagascar associated with faults, these faults results in basaltic flow in southern part of lower indus basin and at the end of cretaceous presence of jurrasic rock shows that deposition occurs during rifting. Because of rifting normal faulting occurs which generates the prominent horst and graben structures. In term of different geologic histories, Pakistan comprises in to two sedimentary basins, Indus basin and Baluchistan basin, which involved in different geologic ages and were combined with each other during cretaceous/Paleocene along Chaman strike slip fault. There is now another smaller basin is identified newly known as Kakar Khorasan basin also refered as Pishine basin. This basin is formed by the convergence of indian and Eurasian plates (Kadri, 1995).

The second large sedimentary basin of Pakistan is Baluchistan basin. It comprises 149,000sq.km onshore area and 8 well have so far been drilled without success. Pishin basin is considered as frontier of oil and gas exploration and it is unexplored basin. Because of anticlinal structure in northern part of Pishin basin it is consider as attractive zone for exploration. Indus basin is the largest and so far the only producing sedimentary basin of Pakistan. The orientation of Indus basin is directed as NE-SW. Due to the interaction between Indian plate and Eurasian plate Indus basin is divided into three parts. These are Upper, Middle and Lower Indus basin and also known as northern, central and southern respectively. Some basement highs present over platform area and these highs are consider as division of Upper, Middle and Lower Indus basin (Riaz Ahmed, 1998). Figure 2.1 shows different sedimentary basin of Pakistan and their division and is discussed below.

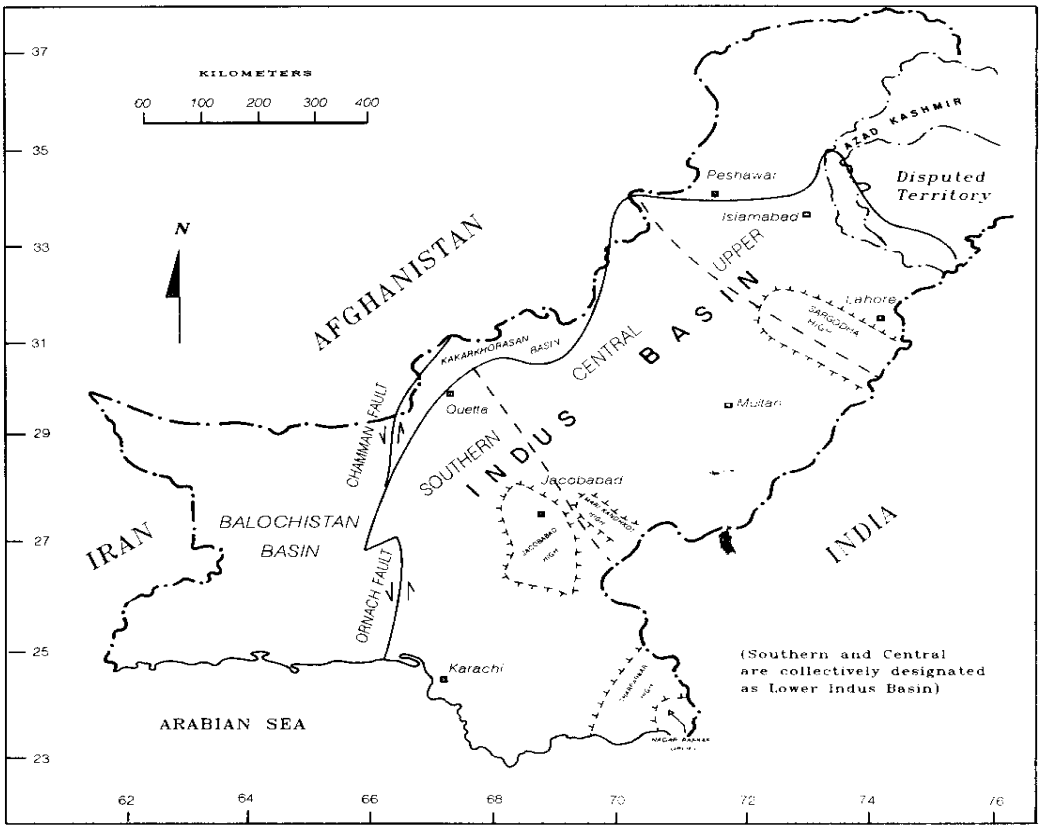

Figure 2.1 Sedimentary basin of Pakistan (Fateh et al., 1984).

Following are the classification of Lower Indus basin:

Lower Indus basin:

- Central Indus basin
- Southern Indus basin

Different classification scheme have been given to the sub-division Lower Indus basin:

Central Indus basin (Sulaiman sub-basin, Raza et al., 1984):

- Punjab platform
- Sulaiman depression
- Sulaiman fold belt

Southern Indus basin (Qadri and Shuaib, 1986):

- Thar platform(Sindh monocline)
- Karachi trough
- Kirthar foredeep
- Kirthar fold belt
- Offshore Indus

Central Indus basin is separated from southern Indus basin along the Jacobabad and Mari-Kandhkot highs and is also known as Sukkur Rift (Raza et al, 1989). Figure 2.2 shows the division of Central Indus Basin and Upper Indus Basin is along Sargodha high. Southern Indus basin lies in the south of Sukkur Rift. Indian shield rock lies in the east of Southern Indus basin and marginal zone of Indian plate lies at its west side. In the south of the Southern Indus basin there is extension which is confined by off-shore Murray Ridg and it is fracture plate boundary (Kadri, 1995).

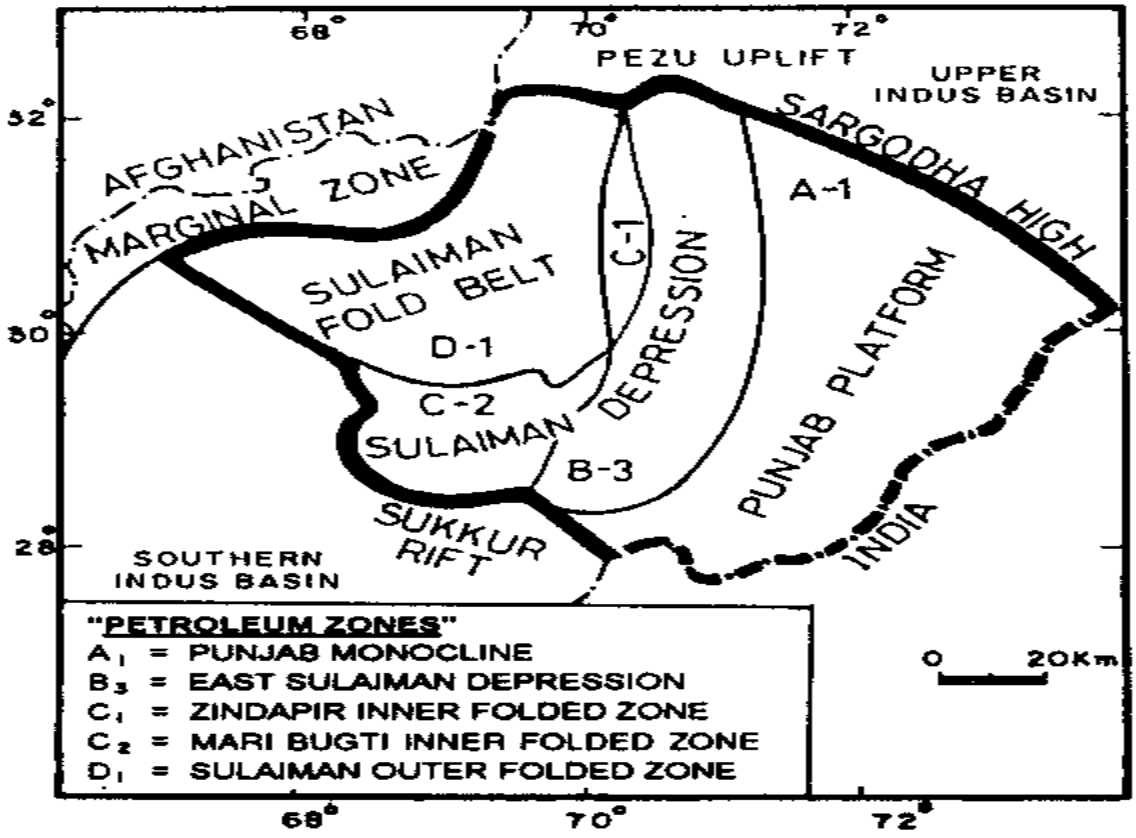

Figure 2.2 Central Indus basin and the subdivision into petroleum zone (Kadri, 1995).

Sindh province is located in Lower Indus basin, and the Miano block-20 area is located among Sindh monocline, Kirthar depression and Mazarani folded zones. This area categorizes its self in both central and Lower Indus basin. In Lower Indus basin Miano is major hydrocarbon producing field with having Lower Goru as reservoir strata.

2.2 Structure and tectonic settings

Tectonically Pakistan consist of two large domain of landmasses known as Tethyan and Gondwanian Domains and is extended in Indo-Pakistan crustal plate. The western and northern area of Pakistan lies in Tethyan Domain and it have complex geological crustal structure, Whereas Indus basin lies in Gondwanian domain and it is consider as much stable zone then other tectonic zones of pakistan (Kazmi & Jan, 1997).

An active continent-continent collision boundary lies in the northeast zone and this boundary is extended up to the west end of the Himalayan orogeny. In the southwest, there is an active sediment and continental sediments, the oceanic part of Arabian plate passing under the Makran arc-trench gap and Afghan microplate (Kadri, 1995).

The Miano block-20 is lies at the division of Central and Southern Indus basin known as Khairpur-Jacobabad high, which is major feature identified on regional seismic lines in the basin. Figure 2.3 shows the tectonic setting of the study area. Deep basement and shallow wrench-tectonic faulting terminated when the K-T (Cretaceous-Triassic) boundary has been established due to uplifting. In Miano area numbers of faults have seen which are normal and strike slip fault which shows that this area lies in extensional regime (Kadri, 1995).

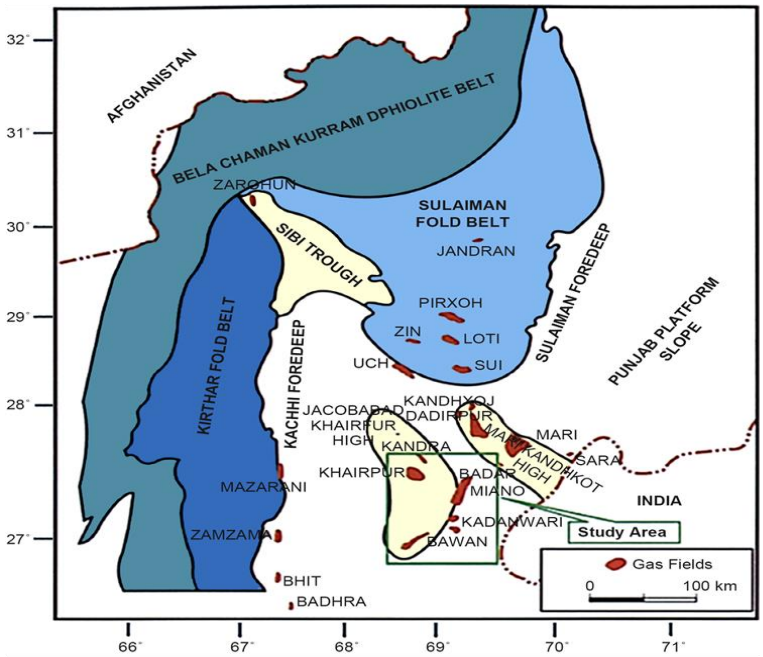

Figure 2.3 Generalized regional tectonic map location of major oil and gas field in the study area (Ahmed et al., 2013).

2.3 Stratigraphy of the area

The distribution of age and the lithologies are shown in a stratigraphic column as shown below in Figure 2.4.

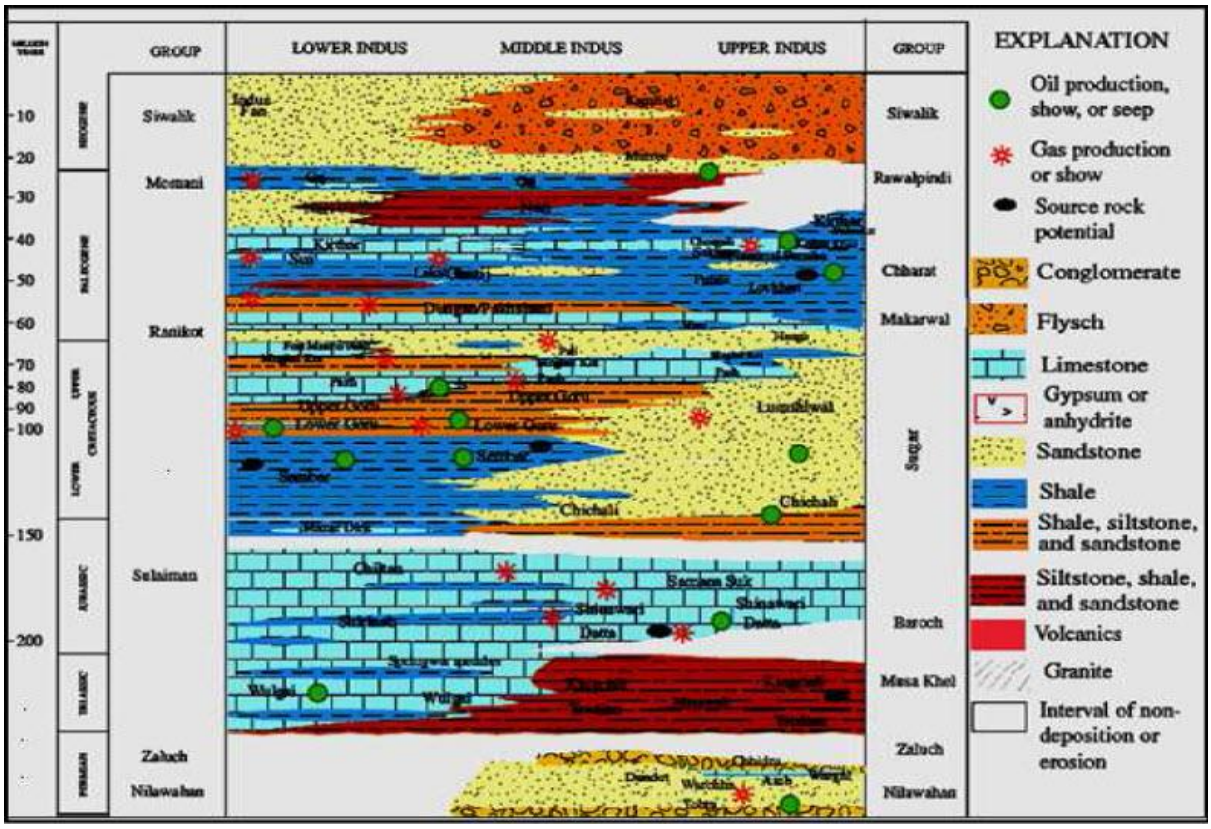

Figure 2.4 Generalized stratigraphic column of Indus basin (www.gsp.com.pk).

Permian to Mesozoic sediments overlying with strong angular unconformity of late Paleozoic age is the sedimentary section of study area. Thick sediments of alluvium deposits are overlain on the whole study area and we cannot directly identify the stratigraphic succession as there is no outcrop lies on the surface. The Mesozoic progradational sequence is deposited on eastward incline gentle slope. Variation in lateral facies from continental shallow marine is represented by prograding time unit directed west to east. Mesozoic sediments are truncated unconformably by volcanic igneous rocks and are regionaly plunging to the west in thar slope area and sedimentary rocks are of Paleocene age.

Inter-bedded siltstone, shale and sandstone of continental to shallow marine lies in permain, jurassic and triassicsedimentry rocks. (Kadri, 1995).The early to middle Jurassic aged Chiltan Limestone in the Middle Indus Basin forms a prominent seismic reflector, which has a smooth planar character. Flattening seismic sections on this horizon helps to remove the complexity of Tertiary structural tilting and faulting, a process that better resolves depositional architecture. The Chiltan Limestone is overlain and down lapped by a Late Jurassic to Early Cretaceous regressive

strata comprising bottom sets, foresets and topsets that prograde towards west from the Indian craton. In lithostratigraphic terms the argillaceous foresets to these prograde are called the Sembar Formation which is an important source rock in the basin. The initial topsets to the prograde have been called the Chichali Formation, while the younger topsets are called the "A" Sand Member of the Lower Goru. No name has yet been given to the sandy submarine fan systems associated with this prograding complex. Sembar Formation is consider as source of hydrocarbon for Lower Indus basin and also for Middle Indus basin. In marine environment it is deposited over Indus basin and its lithology contains black shale with small amounts of siltstone, sandstone. Source of hydrocarbons for most of the Lower and Middle Indus Basins and for the Sulaiman-Kirthar fold and trust belt with TOC's ranging from 0.5 to 3.5 percent in the area. The organic matter in the Sembar Formation is type-III kerogen which is capable of generating gas, but type-II kerogen is also present (Wandrey et al., 2004). The Lower Goru Formation was deposited during the deposition of the latter part of Late Jurassic to Early Cretaceous regressive system. The Lower Goru "A", "B", "C" and "D" sequences were deposited during a gradual and long term 3rd order eustatic or tectonic-eustatic sea level rise. The deposition is punctuated by high-frequency 4th and 5th order relative sea level fluctuations. These fluctuations led to the deposition of prograding clastic sand packages on a vast and widespread ramp. Maintained an overall aggradational packages to slightly progradational profile on "A", "B", and "C" intervals'. The present-day eastward tilt of strata in the study area works with the westwards facies related shale-out of sands to provide stratigraphic trapping of hydrocarbons. In the study area lateral (N-S) shale-out or corrosion in reservoir quality of the "B-sand" reservoir, towards west shale-out of sand to distal settings and to the east structural tilt provide combined structural-Stratigraphic trapping system. (Krois et al., 1998).

2.4 Petroleum prospect

Source, reservoir and trap combine to produce a petroleum prospect. The sand stone of lower goru formation of cretaceous age rock is consider as reservoir portion in the study area. Lower cretaceous rock consist of alternate sand and shale (Khan et al., 2017). These sand consider as reservoir rock unit with change in characterization of reservoir in few kilometer. In Miano area Sember and Ranikot formations act as source rock and the B-interval sand of Lower Goru act as reservoir rock with C-interval which act as topseal.

2.4.1 Source rocks

During the cretaceous time period there is rise in sea level due to which organic life increase. Due to this organic matter preserved over a wide basin. With the passage of time and favorable conditions of temperature and pressure, the preserved organic matter changed into hydrocarbon. Sember, Lower Goru and Ranikot formation contain abundant organic matter which contain characteristic of source rock.

- **Sember Formation:**

Sember Formation is consider as major hydrocarbon source in Lower Indus basin. There is also a large amount of accumulation of gas in Sulaiman range. Hydrocarbon of reservoir ia also present in sand stone of the formation.

Ranikot Formation

Shale of Ranikot formation is consider as main source rock for the presence of gas in the zone, these are the source for overlying Lakhi Formation.

2.4.2 Reservoir rock

In Miano field the sand stone with interbedded shale is the dominant lithology in the B-interval of Lower Goru. The B-interval of Lower Goru formation are the main objective in this prospect. Sandstone is dirty white, and yellowish brown color, medium hard, friable medium grained, sub angular to sub-rounded, sugry, fairly sorted and cemented, argillaceous, visual inter-angular porosity ranged between 10-15%, fair oil shows with scattered and patchy yellowish to bluish white fluorescence and very weak, pale yellowish white residual cut. The thick cretaceous sediments present are good reservoir in the Indus basin. This type of reservoir quality sands are only present in the depositionally up dip, i.e. the shallowest marine part of the lowstand wedge, as are found in the Sawan, Miano and Kadanwari Fields.

2.4.3 Cap/seal rock

There are only structural traps in Southern Indus basin for production. There is no stratigraphic accumulation was found and structural traps are along tilted fault blocks. The structural traps in Lower Indus basin are because of the area lies in extentional regime and also due to horst and graben structures. The cap rock in Lower Indus basin are the thick sequence of sand and shale with underlaying reservoir of Lower Goru.

Chapter 3

Seismic data interpretation

3.1 Introduction

For seismic interpretation data is collected from the Miano (block 20) area. The seismic data must be processed. For better interpretation we have to apply different processing steps on the data (Sroor, 2010). After the seismic processing is done for the selected set of refraction seismic survey lines, data is interpreted. First step is to examine 2D stacked section and to locate possible reflectors.

Interpretation is the main part of petroleum and mineral exploration. Interpretation is the main part of petroleum and mineral exploration. It is the ability of interpreter to decide the place of drill for oil and mineral which is obtained from model of earth by using geophysical data gathered at earth or at the borehole. With the help of stratigraphy and well log data of study area we can do better structural interpretation (Telford et al., 1990).

By using seismic data we can collect information of the earth subsurface with the help of detailed seismic interpretation method. It help us to inderstand the information of study area and location of prospect zone for drilling of well (Coffeen, 1986)

Geologic section give us real picture of subsurface of the area structure vise as well as stratigraphically. This geologic section is obtained by the interpretation which change the seismic section into geologic section (Badley, 1985).

Interpretation combine geophysical and geological information and determine the process involved in seismic wave generation and transmission. The recording equipment effect physical significance of geophysical data. The experience of geological interpreter is important for identification of prospect zone. The geophysical experience require understanding of rock properties, history of the geologic formation and possible structural and stratigraphic trapping mechanism (Lines and Newrick, 2004).

3.2 Interpretation work flow

It is carried out in several steps and different techniques are applied in each step by using software tool. Figure 3.1 shows the procedure adopted for interpretation. It gives the detail information that how dissertation is carried out. First stage is to prepare the base map by loading the navigation data and Seg-y in kingdom software. Faults are marked based on background geologic knowledge about the study area. Then Horizon of interest are marked manually in the software. Then the next step is to generate fault polygons and horizon are contoured to find the high and lows.

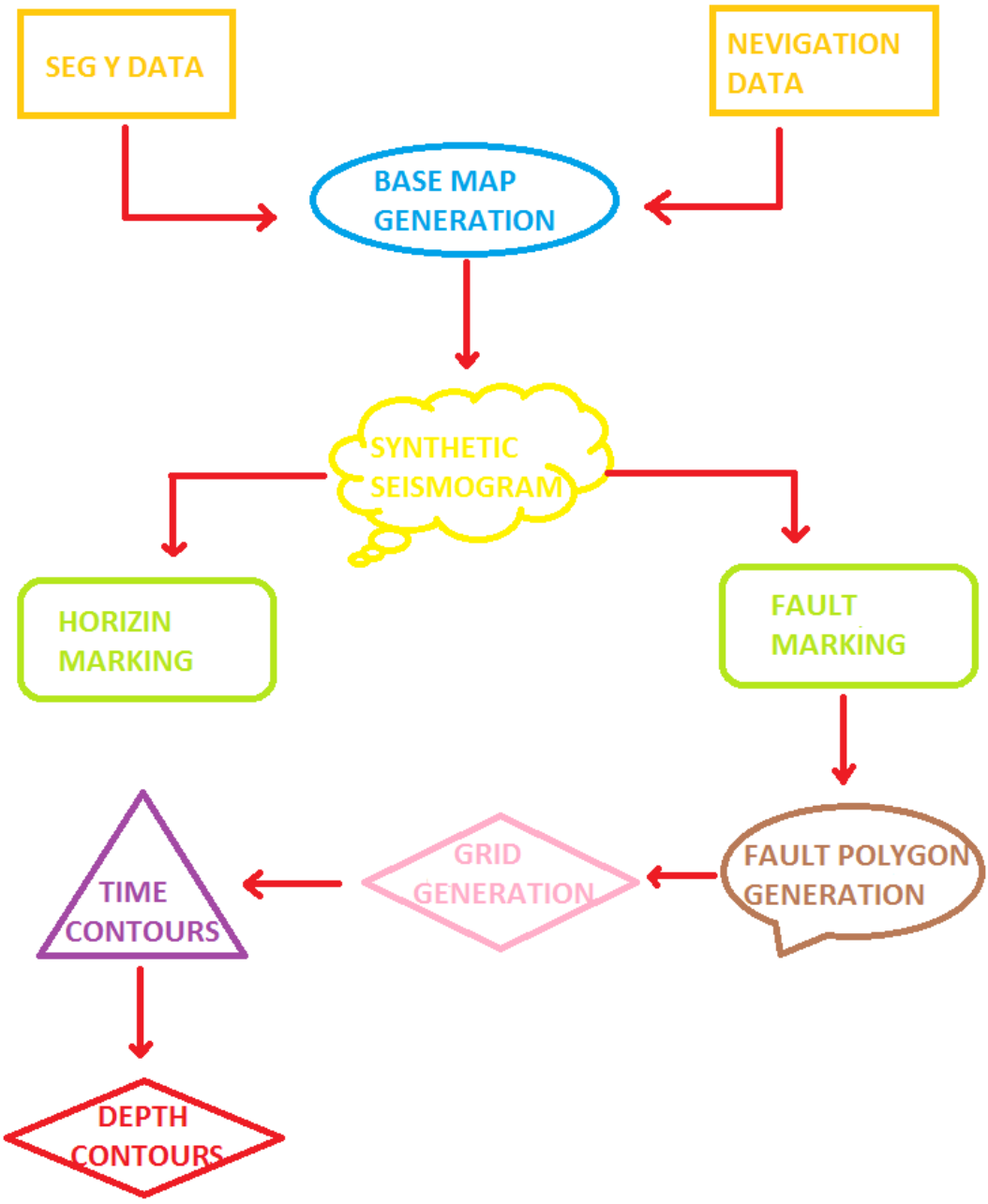

Figure 3.1 Seismic interpretation work flow.

3.3 Base map

For a geophysicist point of view a base map is defined as it is the location of seismic lines and their orientation and shot point at which seismic data were acquired (Sroor, 2010). In base map there is generally the location of well, concession boundaries, orientation of the seismic lines and the seismic survey shot points as shown in Figure 3.2. The base map of study area which contain

two dip line and a strike lines and well position. Dip lines are oriented E-W and strike lines are oriented N-S. Scale bar is also shown on base map and this scale bar is used to determine extent of the line meters on basemap. Shot points are also shown over the lines which are at the interval of 100m.

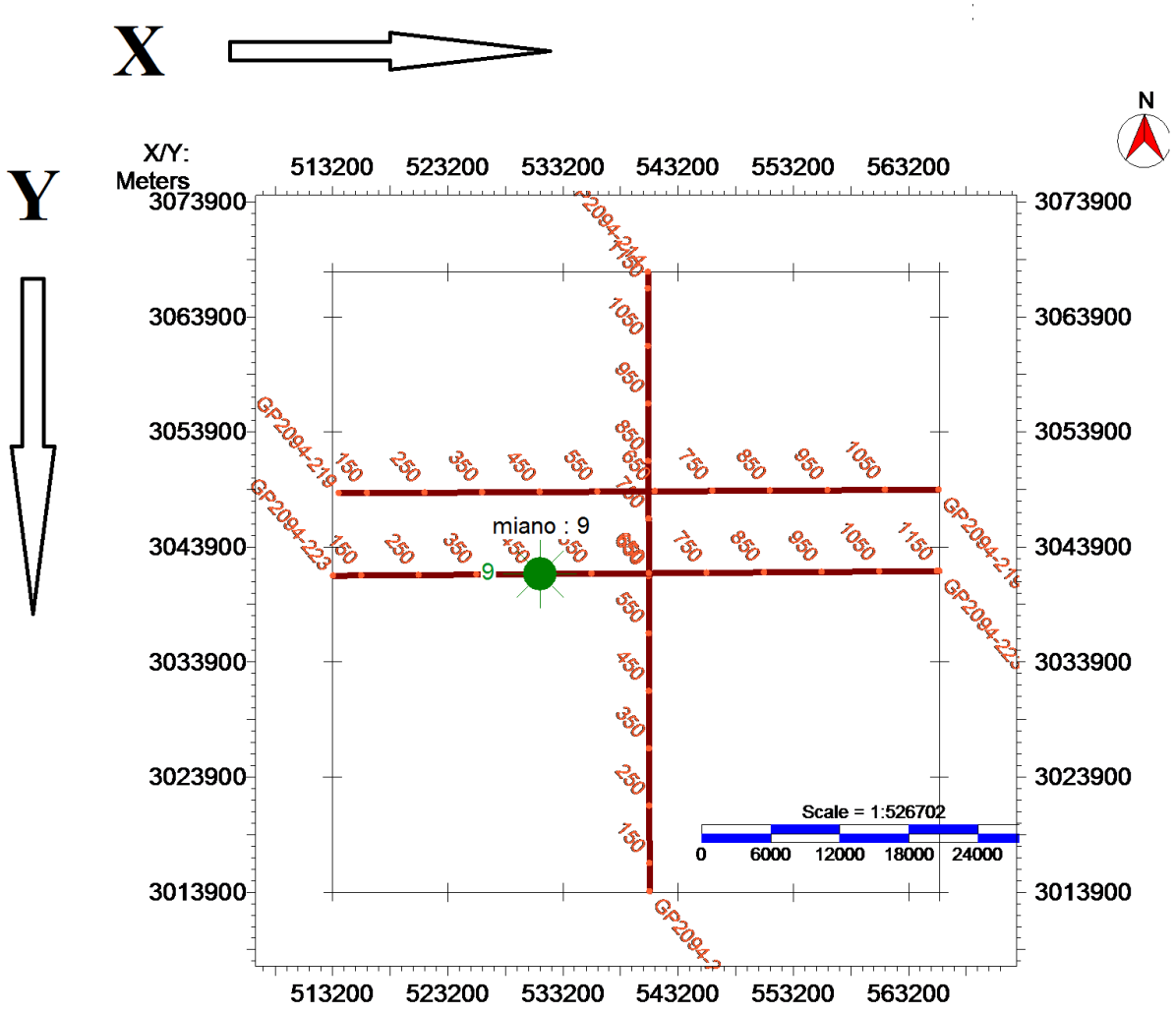

Figure 3.2 Base map.

3.4 Interpretation of seismic lines

For completion of my dissertation I have assigned following lines:

- GP 2094-223 dip line
- GP 2094-219 dip line
- GP 2094-214 strike line

For interpretation structure and stratigraphic knowledge is required (McQuillin et al., 1984). We marked horizon and fault on seismic section. Before marking of horizon synthetic seismogram is

generated at the location of Miano-09 well on the seismic section and we marked the horizon from the information obtained from synthetic seismogram.

3.5 Synthetic seismogram

It is commonly called synthetic and is 1D modelling of acoustic energy moving into the earth subsurface. It is the seismic trace which is used for the correlation with the original seismic reflection. In order to generate synthetic seismogram density and sonic logs are used to produce acoustic impedance then this impedance is converted into reflectivity series and this reflectivity series convolved with the extracted wavelet either from seismic section we get synthetic seismogram. Synthetic seismogram is used to determine that the targeted horizon is peak or trough in seismic section (Sroor, 2010). This information then used to correlate lithologies and age on seismic profile crossing the site. Synthetic seismogram is generated in on Miano-9 well in my study area.

Following are the steps for generation of synthetic seismogram in the software are:

- Load the well.
- Then place the well on seismic line.
- Load formation tops, T_D (time-depth) chart and log curve on the well.
- For velocity used sonic log (DT). Software is automatically using it.
- Now select RHOB (density log) for the density.
- Using a frequency in Hertz in two way travel time.
- Choose a reference log, GR (Gamma Ray) is selected as reference log here.
- Extract traces from nearest seismic line.
- Extract wavelet then convolved with refraction coefficient.

Figure 3.3 shows the synthetic display and only B-interval of Lower Goru formation is confirm with respect to time. Synthetic seismogram is used to mark the accurate location of horizon when tie it with seismic section which is given in time domain but in synthetic seismogram we have formation top in depth domain. From the seismic check-shot survey we get the time and depth values and plot them, then we can extract time values for certain depth (Sroor, 2010).

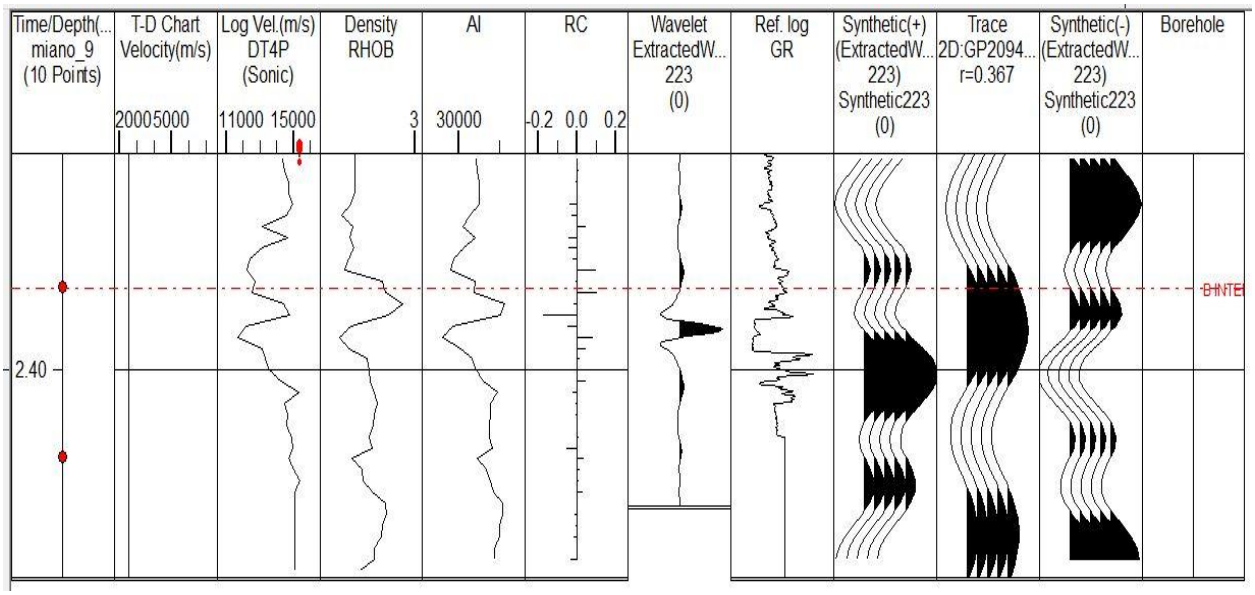

Figure 3.3 Synthetic Seismogram of the well Miano-09 on line GP2094-223.

3.6 Fault identification and Horizons picking

Fault marking on seismic section on real time is quit hard work without knowing the tectonic history of the area (Sroor, 2010). Faults are marked on the basis of discontinuity of reflector. This discontinuity in reflection shows disturbance in the data due to the presence of the fault.

Horizon shows the continuity of reflector in time domain we mark the source, reservoir and cap rock on the seismic section by using synthetic seismogram. Reflection usually crosspond to horizon marking the boundary of different lithology of the rock but does not exactly at the geologic boundary of horizon which is consider as important problem in the interpretation (Kemal et al., 1991).

We picked the interested horizons on seismic lines with the help of synthetic seismogram on the line GP 2094-223 as shown in Figure 3.4. We take the line with well as a refrence line. And this line is used to mark the horizon on other lines. The word (loop) is a tie between inline and crossline. The main purpose of loop is to detect the interested horizon on other line by correlating the two lines with same shot points. If the same event doesn't have the same value then we have to fix the Mis-tie effect by applying shift (Sroor, 2010).

3.7 Interpretation of dip lines GP 2094-223 and GP 2094-219

These are the east-west oriented lines. Figure 3.4 and 3.5 shows the seismic section of dip line GP 2094-223 and GP 2094-219 respectively. We marked the faults and picked the horizons on these seismic sections and their also a well with synthetic seismogram on line GP 2094-223. We picked the horizon which are named C-interval, B-interval, Lower Goru and Ranikot Formation.

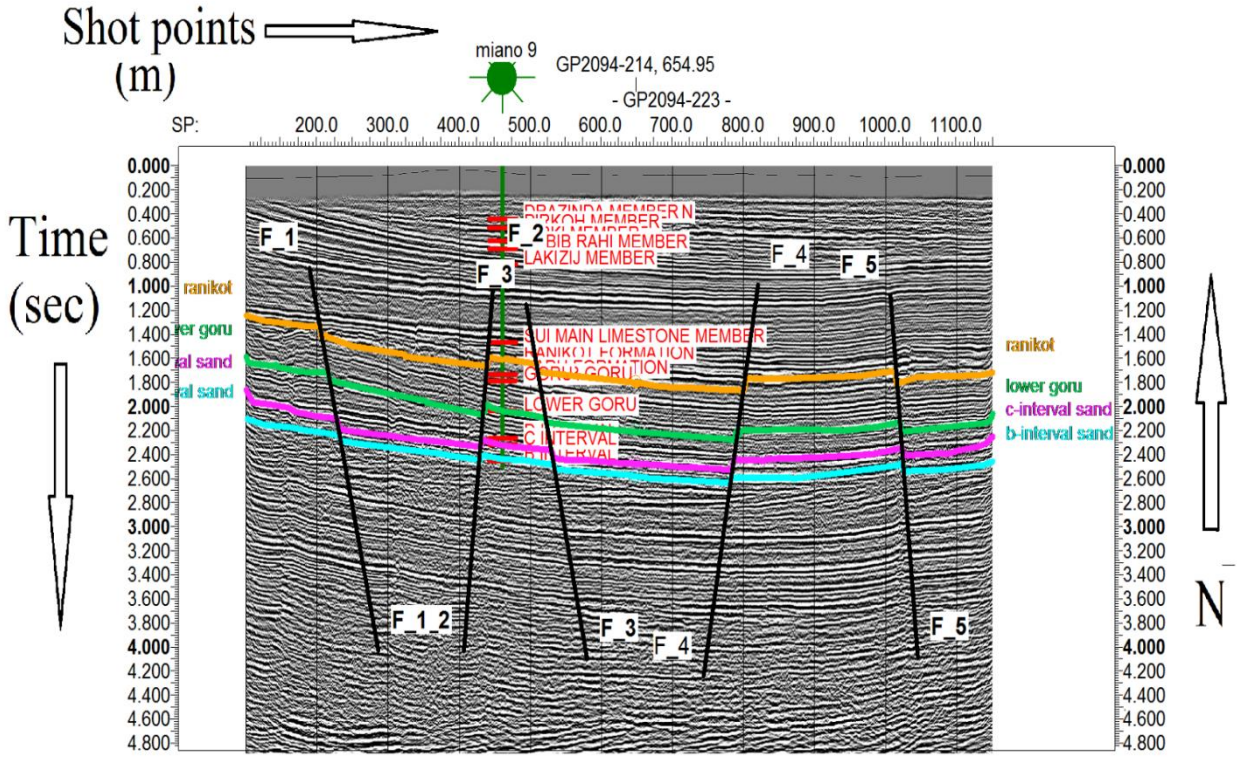

Figure 3.4 Well tie and interpretation of dip line GP2094-223.

Then we mark the horizons on GP2094-219 line by tie GP2094-223 with strike line and then tie the strike line with the GP2094-219, also mark fault on it. The purpose to interpret this line is to confirm the structures which are good for hydrocarbon accumulation.

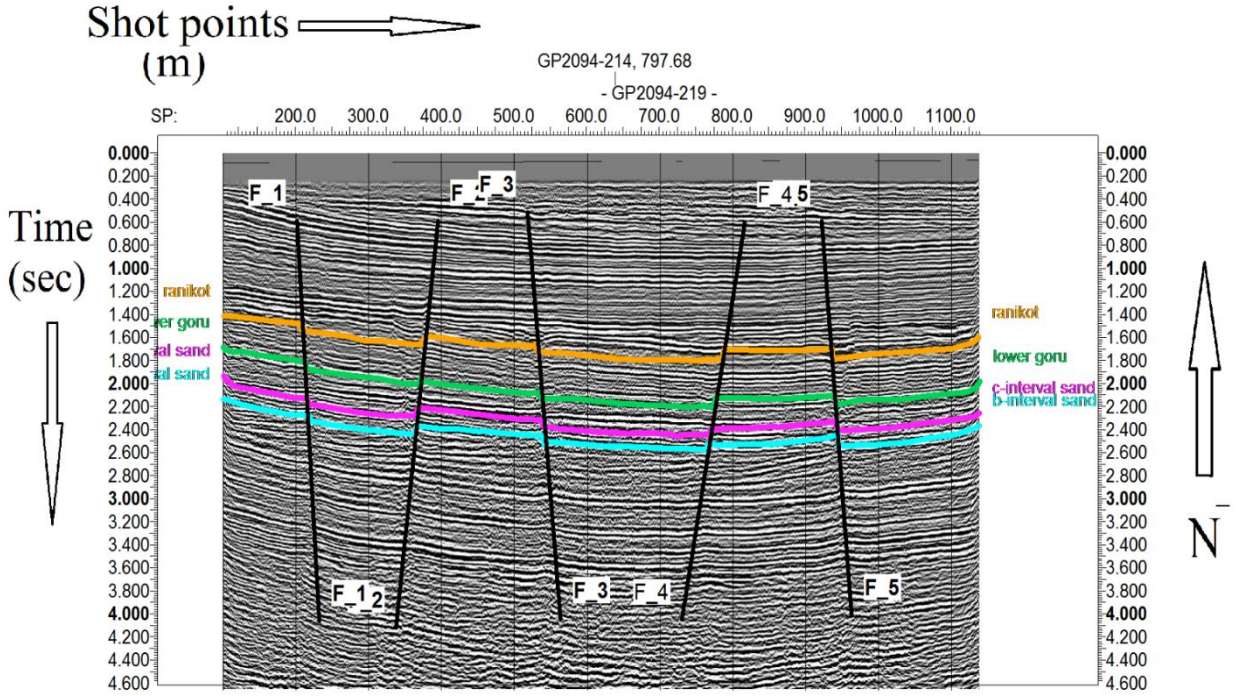

Figure 3.5 Interpretation seismic dip line GP2094-219.

For interpretation there are good structural traps present in this area which are responsible for accumulation of hydrocarbon. There are conjugate normal faulting as shown in above Figure 3.4, 3.5. Due to these normal faulting horst and graben structure are found in this area which are consider as suitable structure for petroleum accumulation. At the place of well location formation are picked at different interval of time and depth as shown in table 3.1. The time of Ranikot Formation is 1.35 second and depth is 1771m. Time of B-interval is 1.61 second and depth is 2551, time of C-interval is 2.08 second and its depth is 3152 m and time of Lower Goru is 2.1706 second and its depth is 33519m.

SN	Formation name	T(sec)	Depth(m)
1	Ranikot Formation	1.35	1771
2	B-interval	1.61	2251
3	C-interval	2.08	3152
4	Lower Goru	2.1706	3319

Table 3.1 TD-chat for the marked Horizon.

3.8 Interpretation of strike line

It is the north–south oriented line. Figure 3.6 shows the strike line GP2094-214 with horizons marked on it. We tie seismic line GP 2094-223 with the strike line GP 2094-214. We apply the shift to remove the Mis-tie and then extend the horizon on the strike line. It is noticed that in order to show the fault on the seismic section the line must be perpendicular to the fault. As strike line doesn't show any fault in in section because it is against the basin configuration.

.

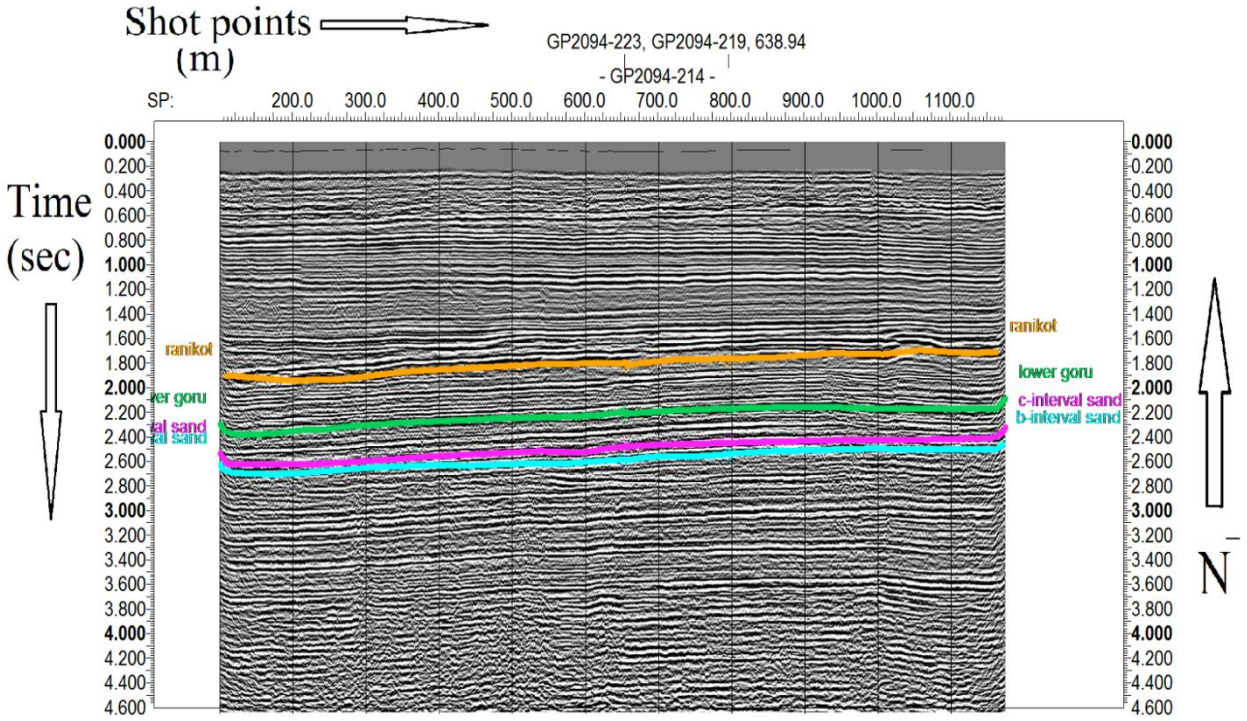

Figure 3.6 Interpretation of the seismic strike line GP2094-214.

3.9 Fault polygon construction

In order to map or contour an area first we have to make fault polygon for that area. Fault which are marked on seismic section are termed as fault segment and the fault which are shown on base map are termed as fault polygon (Sroor, 2010). If the fault does not converted into fault polygon then software can not recognize the discontinuity. As B-interval is acting as reservoir in the study are so fault polygon is generated for B-interval as shown in Figure 3.7. We can confirm the high and low area along the fault by the color bar which is indicating the high and lows of the area.

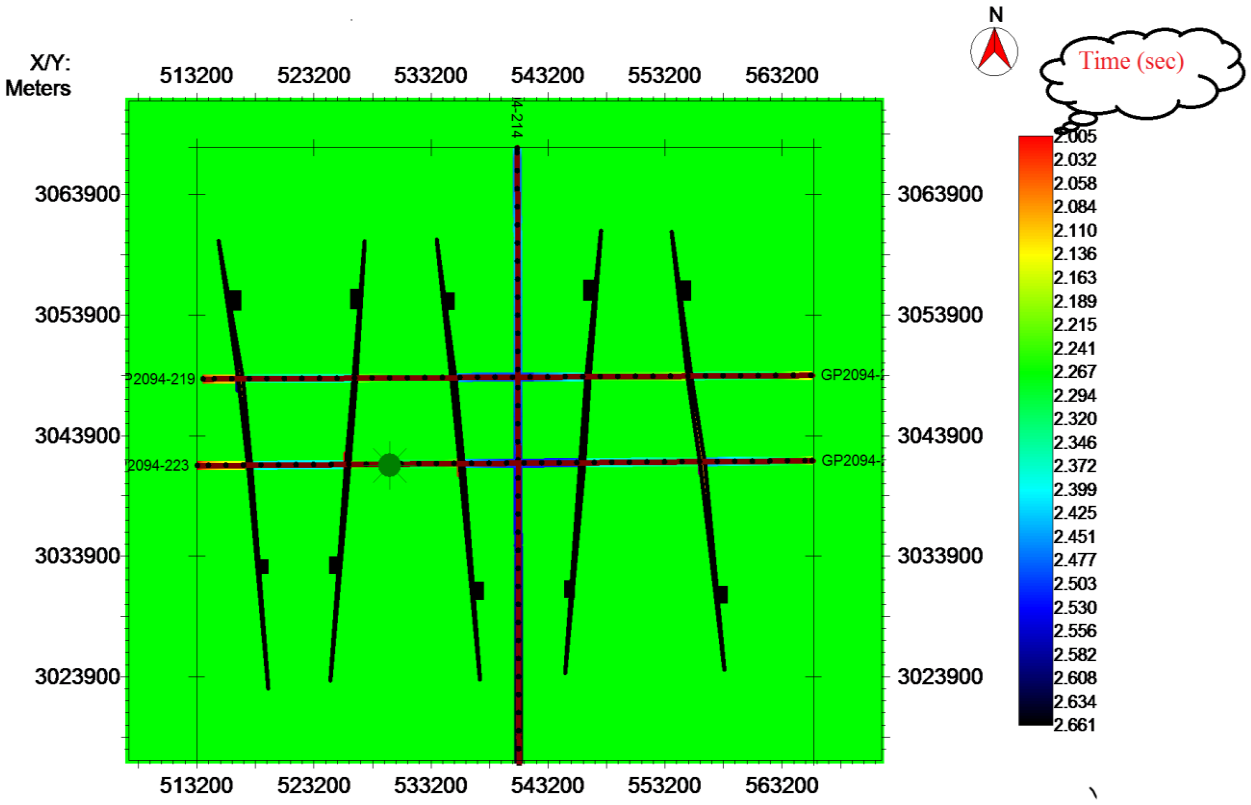

Figure 3.7 Fault polygon constructed at B-interval.

Small rectangles along the fault polygon shows the dip of the fault which are clearly shows the conjugate normal fault. When the fault dip is toward each other than graben is formed and when dip is away from each other horst is formed.

3.10 Contour maps

Contours are the lines of equal elevation around the map as dictated by the data (Coffeen, 1986). Mapping is a part of interpretation of data. This technique help us to see the 3D image of the earth subsurface by constructing contour maps (Osuoji et al., 2013)

- Closing of high contour shows circular shaped body and also indicate upward folding of subsurface. The ring contour having no contour in it referred to as top of up-folded subsurface. Hydrocarbon potential is located in top of the folded subsurface and location of well is also found in this high area.
- Different set of contour which are closing on map shows high and low areas indicate that high area as anticline and low area as syncline and oil and gas accumulation occure in high area.

- Dipping of bed by contour is shown by the increase or decrease in group of contours in specific direction. If the space between the contours decreased this shows steep slop and it is indirect potential zone of hydrocarbon. Oil and gas may be collected in the up-dip.

Seismic maps are produced by contouring seismic data for interpretation which gives us the 3D detail of subsurface various layers. Time and depth contour maps generated with the help of kingdom software.

3.10.1 Time contour map

Time contour map is generated by change in time laterally and vertically for a particular level of horizon. Time contour map is generated for B-interval as it is the reservoir in study area. The contour interval is set 0.025 sec. velocity analysis is done by taking interval velocity from CDP of line GP2094-223 which shows slight change in velocity. From time contour map of B-interval as shown in Figure 3.8 red color shows the lower values of time and blue color show higher values. Color variations clearly shows horst and graben structure. Red color shows shallower part while blue color shows deeper part. In the time contour map the closing of the contours represent the leads. The leads having three types

- One way dip closure (Not bounded by the faults)
- Two way dip closure (one side bounded by the faults)
- Three way dip closure (Two sides bounded by the faults)

In the time contour map of the B-interval all leads which were predicted by the interpretation are two, way dip closure i.e. they have one side bounded by the faults.

Figure 3.8 shows time contour map of the reservoir B-interval. The leads having prospect of the presence of the hydrocarbon. The well Miano-09 is also present on the location of the lead L1 and the Miano-09 is the development well. In the time contour map of the reservoir B-interval all predicted leads are two-way dip closure.

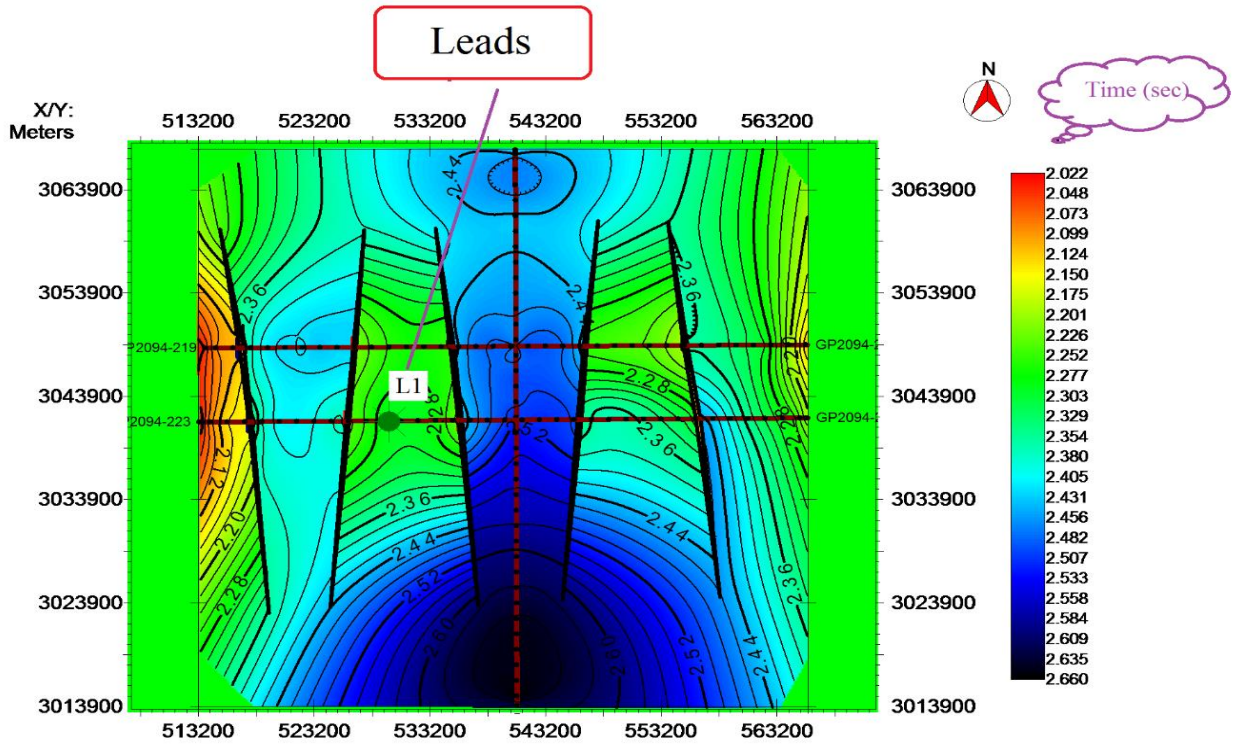

Figure 3.8 Time contour Map of the B-interval of the Lower Goru.

3.10.2 Depth contour map

It shows the variation in direction of particular horizon. Basically, we can constructed depth contour maps by multiplication of one-way with the velocity gradient map. So the times on section is two-way travel time, it must be divided by two before multiplication. A map can be generated by multiplication of velocity with one-way time at each calculated value of velocity data and then contouring is done on their products. Time contour map is converted in to depth contour map using true velocity. For the B-interval we used the 2300m/sec for the depth conversion obtained from the well log data as CDP data is not available to us so we use single average velocity.

The formula used for depth conversion is as follow.

$$s = \frac{vt}{2}\ , \qquad (1)$$

Where S is depth, V is velocity and T is time. Contour interval for depth mapping is 25m. Depth contour map can be prepared by using KB as reference datum. Depth contour map of B-interval is shown in Figure 3.9. It clearly shows the horst and graben geometry. Green color shows the up thrown block while blue color shows down thrown block.

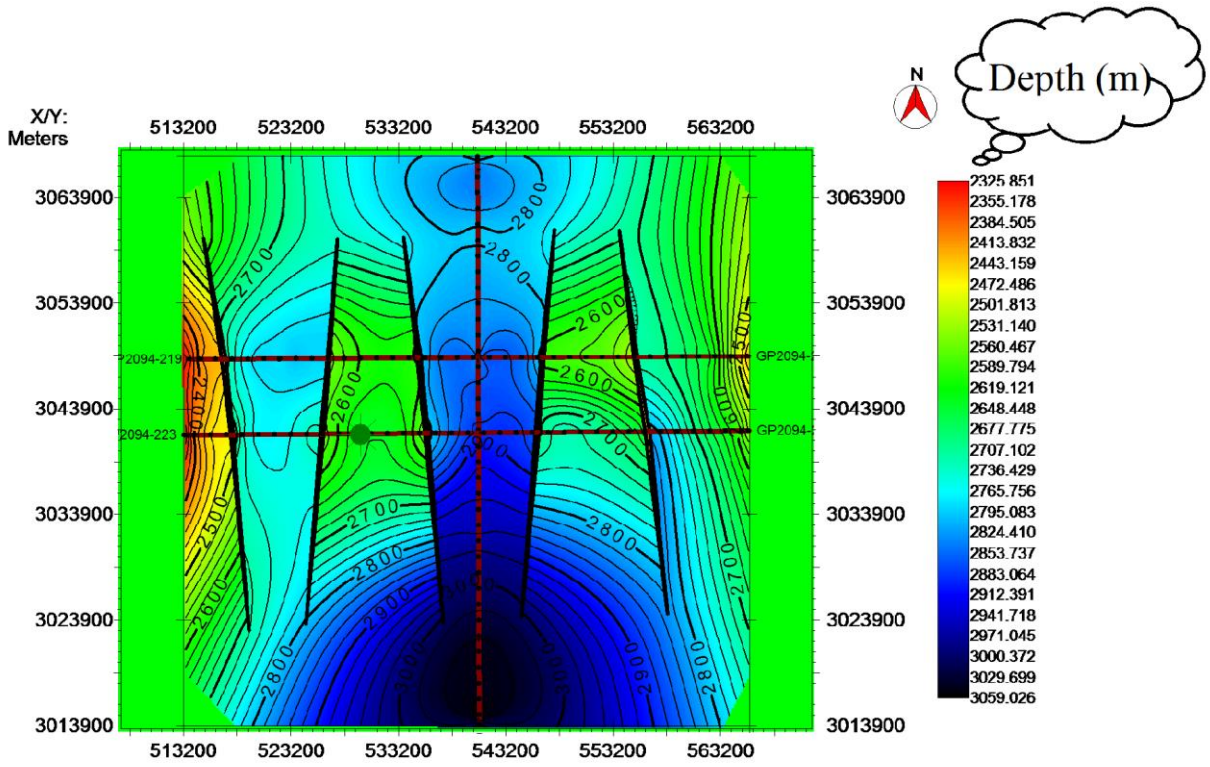

Figure 3.9 Depth contour Map of the B-interval of the Lower Goru formation.

3.11 Seismic attributes

3.11.1 Introduction

"Seismic Attributes gives all the information obtained from seismic data, either by direct Measurements or by logical or experience based reasoning." (Taner, 2000). Number of attributes defined in order to the exploration of seismic. Most of the attributes have been used for interpretation and analysis of seismic data (Chopra et al., 2005). Some particular attribute applications are considered i.e. Amplitude, Frequency and Energy.

Seismic attribute help in measuring of seismic data for better interpretation to analysis features of intrest. It is consider as very important tool for accurately determine the development and prediction in exploration of hydrocarbon. We can interpret different features like faults and channels and determine their depositional environment and the history of the formation of different structures. Seismic data also help in determination of seismic data quality to understand the characteristics of reservoir and to identify the prospect. Seismic attributes also help in enhancement of different features by Combining information with adjacent seismic samples and traces using a physical model (such as dip and azimuth, waveform similarity, or frequency

content), so that it can easily be interpreted by human and also by the modern geostatistical computer analysis. Lateral changes in geology and also in noise are sensitive to seismic attribute (Oyeyemi and Aizebeokhai, 2015).

3.13 Classification of Seismic Attributes

The Seismic Attributes have been evolved into two categories.

- Physical Attributes
- Geometric attributes

(A) Physical Attribute

We can estimate physical qualities and quantities through physical attributes. It gives pertinent information which help in reservoir characterization and lithology identification. The trace envelope is sensitive to acoustic impedance contrast, frequencies attribute is sensitive to the thickness of bed, wave scattering and absorption. Instantaneous phase attribute is directly relate to rock properties. (Taner, 1994).

(B) Geometric Attribute

Geometrical attributes determine the temporal and spatial relationship with other attributes. They also determine Lateral continuity which gives good indication of bedding similarity and also discontinuity. Depositional information is obtained by dip and curvature of bedding. Stratigraphic interpretation is done by geometric attributes which are better indication of different characteristics of event and also used to recognize depositional pattern and quantify different feature of interests (Subrahmanyam, 2008).

3.14 Envelop of Trace (Reflection Strength/ Instantaneous Amplitude)

Envelop trace attribute is commonly known as reflection strength. It is the representation of instantaneous energy of complex trace and it is not dependent of the phase and is computed as the modulus of the complex trace as given below (Chopra et al., 2005),

$$A(t) = \sqrt{q^2(t) + r^2(t)}\,, \qquad (2)$$

The envelope directly related to the acoustic impedance contrasts. We can see separate boundary contrast and also combined response of several boundary which depend upon seismic band width. Figure 3.10 shows the real, imaginary and envelope trace. It can be observed that the envelope trace always remains positive. This attribute is computed for seismic line GP 2094-219 as shown in Figure 3.11 which clearly shows the reflection strength of marked reservoir zone. It shows high amplitude with yellow color while brown color shows low amplitude values. Shale is indicated by high amplitude values. This attribute is used for identifying (Chopra et al., 2005),

- Gas accumulation shown by Bright spots.

- Major changes of lithology.
- Local horizontal change indicating faulting.

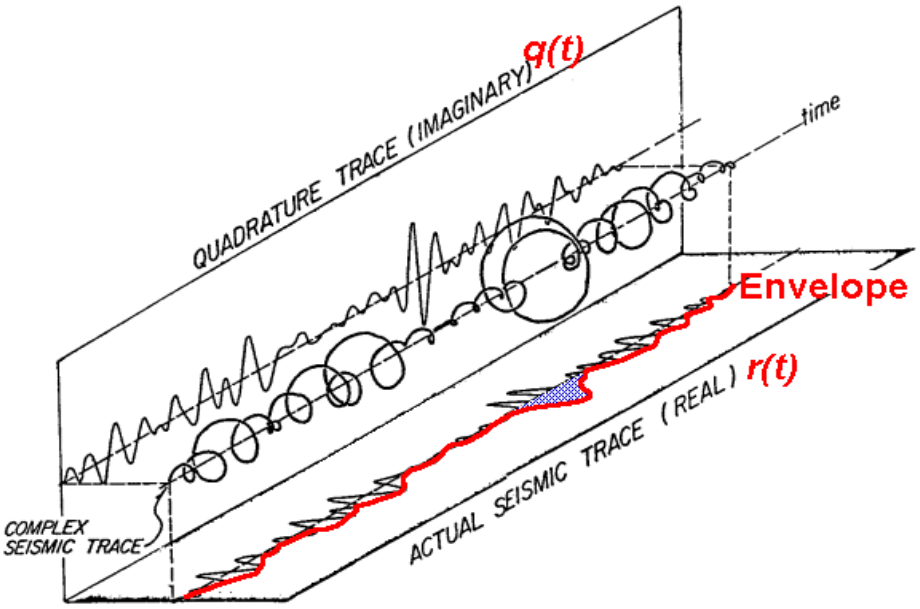

Figure 3.10 An envelope trace is contributed for real seismic trace (Taner etal., 1979).

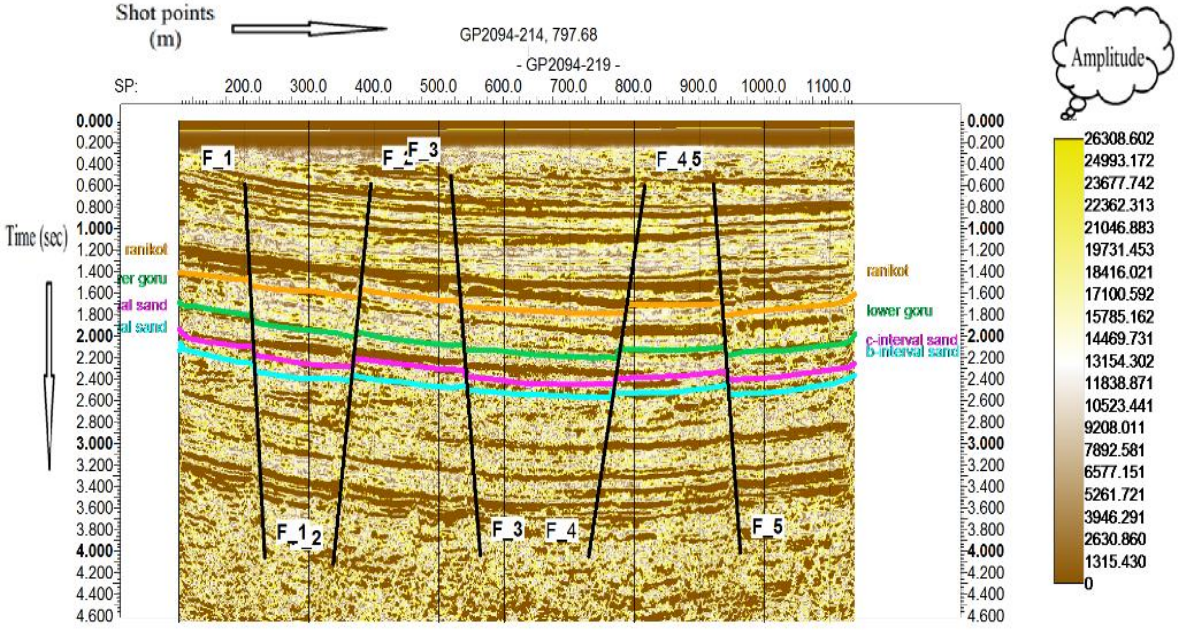

Figure 3.11 Trace envelop attribute on line GP 2094-219.

3.15 Instantaneous phase

Phase attribute is a physical attribute. Geometric shaped classifications can easily be identified by this attribute. The phase information is independent of trace amplitudes and relates to the

propagation of phase of the seismic wave front. Figure 3.12 shows clearly the continuity of reflector on line GP 2094-219, this attribute is independent of the amplitude.

This attribute is useful as (Subrahmanyam, 2008),

- Instantaneous phase gives the excellent indication of lateral continuity of reflector.
- It can be used to highlight interface in sections with high decay of amplitudes and even highlight deeper horizons which are not visible in the normal amplitude sections.
- Shows discontinuities.
- Detailed visualization of bedding configuration.

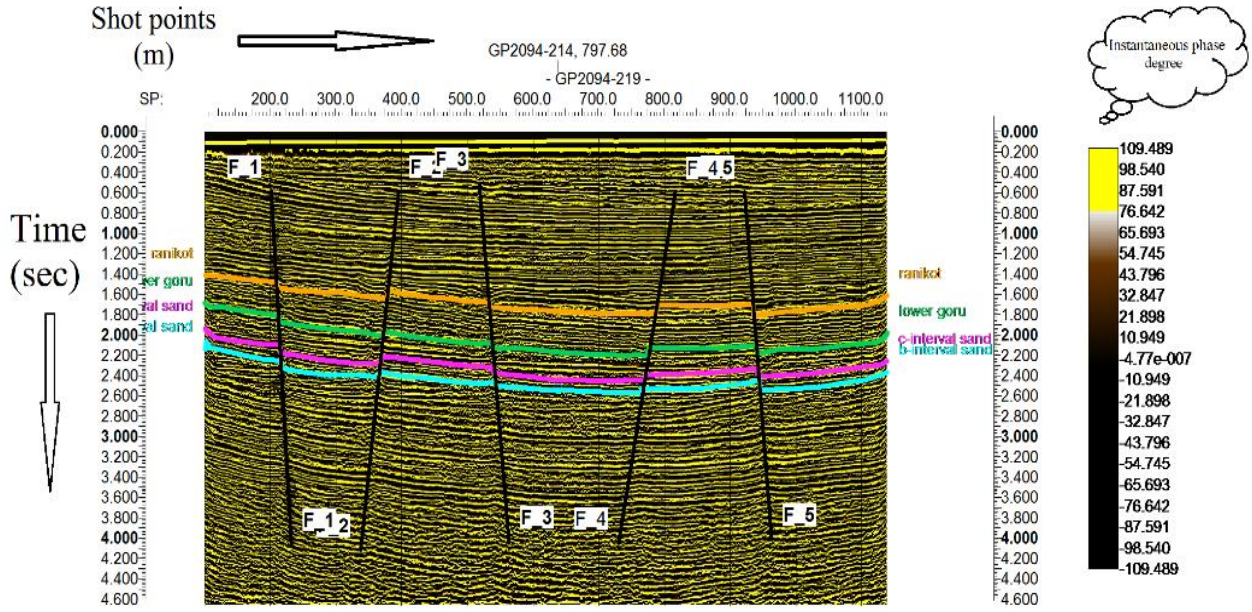

Figure 3.12 Instantaneous phase attribute on line GP 2094-219.

Chapter 4

PETROPHYSICS

4.1 Introduction

Our discussion in this chapter is about the hydrocarbon reservoir in the study area. Geological and geophysical studies help us to understand the presence of reservoir in subsurface. Reservoir are characterize with the wire line log and mud logging data of Miano-09 which is been selected for reservoir characterization. Petrophysics is one technique used for the reservoir characterization. This study facilitates in identification and quantification of fluid in a reservoir (Ali et al., 2014).

The aim of petrophysics is determination of physical properties like porosity, saturation, permeability and closely related to production perimeter and also determine net pay, fluid content, and shale volume and reservoir zone. It uses data from different geophysical tool, this data is then used for determination of properties of subsurface of earth.

In Petrophysical analysis we get the detailed information from all the log, core and wire line log data and it help in derivation of above defined properties with maximum accuracy. Petrophysics technique is widely used by Petroleum Engineers, Well Log Analysts, Core Analysts, Geologists and Geophysicists (Dewar and Pickford, 2001). Petrophysical interpretation has less concern with the seismic and more concerned with using well bore measurements to contribute to reservoir description (Krygowski, 2004).

4.2 Data set

Reservoir characteristics are determined by Petrophysical analysis of Miano area. We use the log data from Miano-09 well to compete the aim. The log curves from this borehole used are:

Caliper log, , Gamma ray (GR), Sonic log (DT), Spontaneous potential log (SP), Deep laterolog (LLD), Shallow laterolog (LLS), Neutron log (NPHI), Density log (RHOB). For Petrophysical analysis, using the well log curves we calculate the following parameters.

1. Volume of shale
2. Porosity (average porosity and effective porosity)
3. Water saturation
4. Hydrocarbon saturation

4.3 Classification of Geophysical well logs

There are three basic log tacks which are as follow:

- Lithology log track
- Resistivity log tack
- Porosity log track

4.4 Lithology log track

In lithology log track we put three logs which are as follow:

- Gamma ray log (GR)
- Caliper log
- Spontaneous potential log (SP)

4.4.1 Caliper log

It is a well logging tool, it provides information about borehole size and shape and depth. It is used for exploration of hydrocarbon during drilling of wells. The log measurements are very good indicator of shale, swelling in the borehole and cave-in, which cause deviation in other well logs records. Higher values show the shale material and lower values show sandstone.

4.4.2 Gamma ray log

Gamma ray are the lithology log. This log measure the natural radioactivity of the formations. Gamma radiations are emitted in the form of electromagnetic energy called photon. When photon collides with electrons, some energy is transferred to electron called Compton scattering. These scattered radiations reached the detector and are counted after absorption of gamma rays from natural radioactive source present within the layer. These emissions are counted and displayed as count per second which is termed as gamma ray log. This log is very important and used for various purposes however, its basic purpose is to differentiate between sand and shale (Asquith and Gibson, 2004). Shale have radioactive material present in it which shows high Gamma ray readings, whereas the sand and other carbonates have low Gamma ray readings.

4.5 Resistivity log track

There are number of different resistivity logs, which gives us the information about the thickness of the formations, and is known as principal indicator of hydrocarbon. These type of log are plotted on logarithmic scale due to variation in resistivity with depth. The resistivity log which are given in my data are:

- Deep laterolog (LLD)
- Shallow laterolog (LLS)

The Dual Laterolog Tool is used to measure the formation resistivity in boreholes with highly conductive drilling mud, or where there is a huge contrast in the mud resistivity and formation resistivity. The DLL produces two measurements, the laterolog shallow (LLS), and laterolog deep (LLD). When combined with a microspherically focused tool (MSFL), a resistivity profile with three depths of investigation is possible.

4.5.1 Deep laterolog

The deep laterolog (LLD) is used for measurement of formation resistivity at greater depth. The effective depth of investigation is depends on the extent to which the surveying current focused

(Asquith and Krygowski, 2004). It provides strong focusing deep into the formation.
This log is used for saline muds and also in case of fresh mud. It is also used to determine Rt.

4.5.2 Shallow laterolog

It is used for measurement of resistivity of invaded zone (Ri). In water bearing zone the shallow laterolog records a low resistivity because mud filtrate resistivity (Rmf), which is nearly equal to mud resistivity (Rm) (Asquith and Krygowski, 2004).

4.6 Porosity log track

In porosity log track we have logs which are helpful to determine the porosity of the interested zone and to determine the presence of oil, gas and water. Porosity is defined as the ratio of volume of spaces to the total volume of rock (Bell, 2013). We can calculate the Porosity for different zone using following log data, which are sonic/DT log, neutron log (NPHI), density log (RHOB).

4.6.1 Sonic log

The sonic log is tool for measurement of the time of wave travelling through the formation. This time is then used to calculate the velocity of waves travelling through different formation. Its aim is to give information about the seismic data and calculate the porosity of formations. Sonic log can also be used for the following purposes in combination of other logs as given by (Asquith and Krygowski, 2004).

- Record the information of travel time and velocity through borehole. This information can be used to calibrate a seismic data set (i.e., tie it in to measured values of seismic velocity).
- Use information from seismic data and creating synthetic seismograms.
- Facies recognition.
- Determination of porosity.
- Fracture identification.
- Identification of lithologies.

Frequency is high in sonic logging tool then seismic wave so we have to be careful in direct comparison and application of sonic log data with seismic data.

4.6.2 Density log (RHOB)

It is the measurement of density of electron in the formation. The logging device emits gamma rays these gamma rays then collide with the electrons of the formation. These gamma rays then scattered and reflected, number of the reflecting gamma rays are received at the detector which are indicative of bulk density of formation (Dan J. Hartmann and Edward A. Beaumont). Density log with other logs and separately for different purposes (Tittman and Wahal, 1965).

4.6.3 Neutron log (NPHI)

The neutron log depends on number of hydrogen atoms present in the formation. Its aim is to determine the porosity. This logging tool operates by bombardment of high energy neutrons with the formation. These high energy neutrons scattered by the formation, here the energy is loss and gamma rays with high energy are produce. If hydrogen atoms present in the formation very effective scattering reaction will occurs. This result in neutron with low energy and amount of hydrogen atom present in the formation define the count rate of neutron (Dr. Paul Glover). As the concentration of hydrogen ion is less in the gas as compare to water and oil that's why porosity measured by the neutron log is low then the true porosity of the formation (Asquith and Krygowski, 2004).

4.7 Scale used for different log curves

The scale which are used in different log tracks and their units are shown in Table 4.1. scale of Gamma ray Log range from 1 to 300 API, Caliper Log range from 6 to inches, Sonic log values range from 140 to 40 μsec/ft, Density Log range from 1.95 to 2.95 Gm/Cm3, for Neutron Log Values range from 0.45 to -0.15 PU. The range of LLD and LLS range from 1 to 1000 Ωm.

Sr #.	Log name	Scale	Unit
1	Gamma ray Log (GR)	0----------300	API
2	Caliper Log (CALI)	6----------16	Inches
3	Sonic Log (DT)	140----------40	μsec/ft
4	Density Log (RHOB)	1.95---------2.95	Gm/cm3
5	Neutron Log (NPHI)	0.45---------(-0.15)	PU
6	Laterolog Deep (LLD)	1----------1000	Ωm
7	Laterolog Shallow (LLS)	1----------1000	Ωm

Table 4.1 Scale used for different log curves for Petrophysics.

4.8 Workflow for petrophysics

Petrophysics interpretation work is carried out on kingdom software. There are different steps which are applied to find different properties of rock. Figure 4.1 shows the workflow adopted for petrophysics. In first step log data of Miano-9 well is loaded on kingdom software. Then we find shale volume, porosity, effective porosity, water saturation and hydrocarbon saturation using these loaded log data by applying different equations.

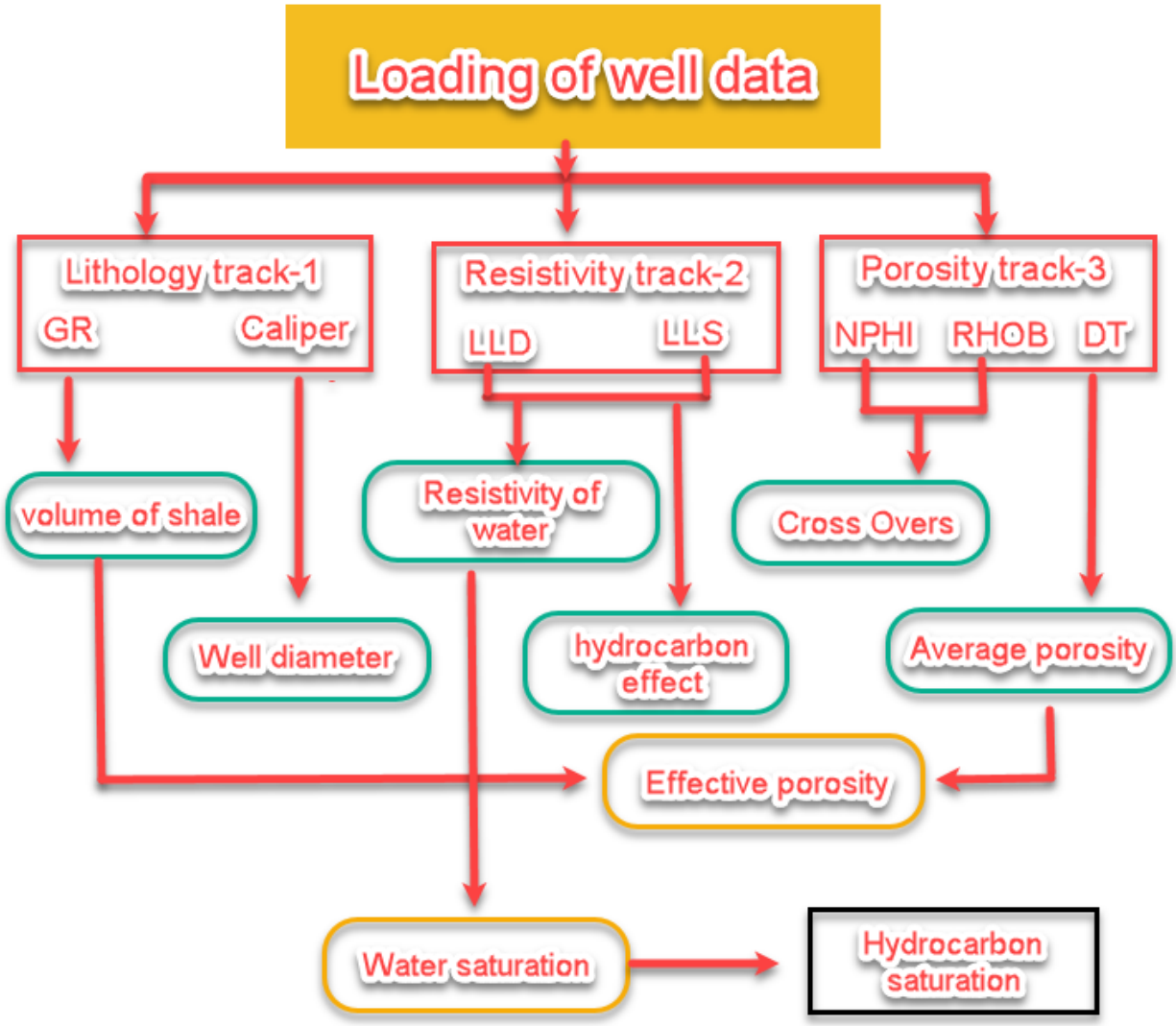

Figure 4.1 Workflow for petrophysics interpretation.

4.9 Calculation for volume of shale

GR log is used for calculation of shale volume. Shale is more radioactive than carbonate or sand, and are indicated by higher Gamma ray values. The formation which are termed as clean formation are assumed that they do not contain radioactive material. This creates a contrast between shale and other formation. The mathematical formula for calculation of volume of shale is given below (Asquith and Gibson, 2004).

$$I_{GR} = \frac{GR_{log\_} GR_{min}}{GR_{max} - GR_{min}} \quad , \qquad (1)$$

Where I_{GR} is Gamma ray index, GR_{log} is Gamma ray reading of the formation, GR_{min} minimum value of Gamma ray (clean sand and carbonate), GR_{max} is maximum value of Gamma ray (shale).

4.10 Calculation of porosity

The pore spaces which are not occupied by the rock fragments are named as porosity. Porosity is generated in the rock by dissolution process and also by fracture in rock. Porosity is represented by symbol "Ø" and it is expressed percentage as well as in decimals. The primary porosity is formed during the time of deposition of sediments and pore spaces which are formed due to fracturing and dissolution is known as secondary porosity. We can calculated porosity using following methods:

Density log is used for derivation of density porosity by the following equation (Asquith and Gibson, 2004).

$$\emptyset_{\mathrm{d}} = \frac{\rho_{\mathrm{m}} - \rho_{\mathrm{b}}}{\rho_{\mathrm{m}} - \rho_{\mathrm{f}}}, \quad (2)$$

Where $\emptyset_{\mathrm{d}}$ is density porosity, ρ_{b} is bulk density of the formation, ρ_{m} is density of matrix, ρ_{f} is Density of fluid (salt mud =1.1 & fresh mud =1.0).

Neutron porosity is directly obtained from neutron log. Sonic porosity can be calculated by using formula Wyllie in 1958.

$$\emptyset_{\mathrm{s}} = \frac{\Delta t_{\mathrm{log}} - \Delta t_{\mathrm{m}}}{\Delta t_{\mathrm{f}} - \Delta t_{\mathrm{m}}}, \quad (3)$$

Where $\emptyset_{\mathrm{s}}$ is sonic porosity, Δt_{log} is interval transient time of formation, Δt_{m} is interval transient time of matrix, Δt_{f} is interval transient time of fluid (fresh mud =189 &salt mud =185). Increase in the interval transient time of formation in the presence of Hydrocarbon known as effect of hydrocarbon. This effect has to be removed, if not then sonic porosity may be too high.

4.11 Average porosity

We can calculate the Average or Total porosity by adding all the porosities calculated by logs and divide by number of logs used. We calculate the average porosity for reservoir, which is the Lower Goru sand of cretaceous. The relation is given below for calculation of average porosity.

$$\emptyset_{avg} = \emptyset_d + \emptyset_s + \emptyset n \quad (4)$$

Where $\emptyset_{\mathrm{avg}}$ is average porosity, $\emptyset n$ is neutron porosity, $\emptyset_{\mathrm{d}}$ is density porosity and $\emptyset_{\mathrm{s}}$ is sonic porosity.

4.12 Effective porosity

Effective porosity is defined as interconnectedness of pores from which shale effect is removed. Water saturation is calculated by using effective porosity in reservoir zone. Formula for calculation of effective porosity is given in equation below.

$$\emptyset_e = (1 - \mathrm{Vsh}) \times \emptyset_{\mathrm{avg}}, \quad (5)$$

Where $\emptyset_e$ is effective porosity, Vsh is volume of shale and $\emptyset_{\mathrm{avg}}$ is average porosity.

4.13 Calculation of water saturation

Water saturation is defined as the volume of pores contain by how many parentage of water. To determine the water and hydrocarbon saturation is the major role of petrophysical analysis. For water saturation calculation, Archie develop an equation which is,

$$S_w = \sqrt[n]{\frac{F \times R_w}{R_t}} \quad , \qquad (6a)$$

Where S_w is water saturation, R_w is resistivity of water, Rt is true resistivity, F is formation factor and formation factor is calculated as

F= $\frac{a}{\emptyset^m}$

Where “a” is constant and its value is 1 in case of sand, ”∅" is the effective porosity and “m” is the cementation factor and its value is 2 for sandstone.

For RT we take LLD log readings, and for Rw there are following steps.

The value of SP value at maximum depth of deflection provides value of SSP by calculation given below in equation.

SSP = SP(sand) – SP(shale) , (6b)

Where SSP is static spontaneous potential, SP (sand) is spontaneous potential for sand and SP(shale) is spontaneous potential for shale. Calculate the formation temperature (FT) from the relation given below also defined by Archie.

$$\text{FT} = \text{BHT} - \text{ST} \times \frac{\text{FD}}{\text{TD}}, \qquad (6b)$$

Where FT is formation temperature, BHT is borehole temperature, FD is formation depth, TD is total depth and ST is surface temperature. Now after calculation of FT calculate the mud filtrate resistivity at the zone of interest (FT) by using following relation.

$$R_{mf2} = \frac{(\text{ST}+6.77) \times R_{mf1}}{(\text{FT}+6.77)}, \qquad (6c)$$

Where R_{mf2} is the resistivity of mud filtrates at surface temperature, ST is surface temperature, R_{mf1} is resistivity of mud filtrate at formation temperature and FT is formation temperature.

4.14 Calculation of hydrocarbon saturation

Hydrocarbon saturation is defined as the percentage of pore spaces contain hydrocarbon. Mathematically it is given by the following equation.

$S_{hc} = 1 - S_w$ (7)

As the S_{hc} is the remaining percentage of the pore volume occupied by Water, hence this method is indirect quantitative estimation of the hydrocarbons.

4.15 Petrophysical interpretation of Miano-09 well

We can interpret the well logging by examine the different behavior of the log curves. The first log track is about lithology we have caliper log and GR log, caliper help to determine the correct reading of the other log as shown below. We have GRlog which is used to determine the shale, if log shows high values then high will be the percentage of shale at that point and we can easily define the shale free zone where GRlog value is minimum. We can predict that this shale free zone contain hydrocarbon. To confirm the type and quantity of the hydrocarbon we will see other logs. Then in second track we have resistivity log used to determine the quantity of water, oil or gas. LLD and LLS log curve are present here, if there is a separation between them, then this shows the reservoir zone. High value of LLD shows hydrocarbon whereas low values shows water saturation. Then in third log track we have different porosity logs, if we see the crossover of NPHI and RHOB log curves then this area indicates reservoir zone. Larger the crossover indicate gas, smaller crossover shows the presence of oil and the overlapping of these two logs shows the presence of water. Then DT log in third track help to calculate sonic porosity which is shown in fourth track as shown in Figure 4.2. We have average porosity and effective porosity in track five and six respectively. Porosity play a major role in reservoir identification and also the quantity of the reservoir fluid. Then we have water saturation and hydrocarbon track. We have to mark the interested zone where there is small quantity of water and relatively greater amount of hydrocarbon. If the hydrocarbon is present much enough for the economic point of view then we will drill for exploration. Petrophysics interpretation is done for B-interval from depth 3331 to 3385. We see that the zone from depth 3338 to 3346 is indicator of gas reservoir zone. It fulfill the criteria for the gas reservoir which is discussed above.

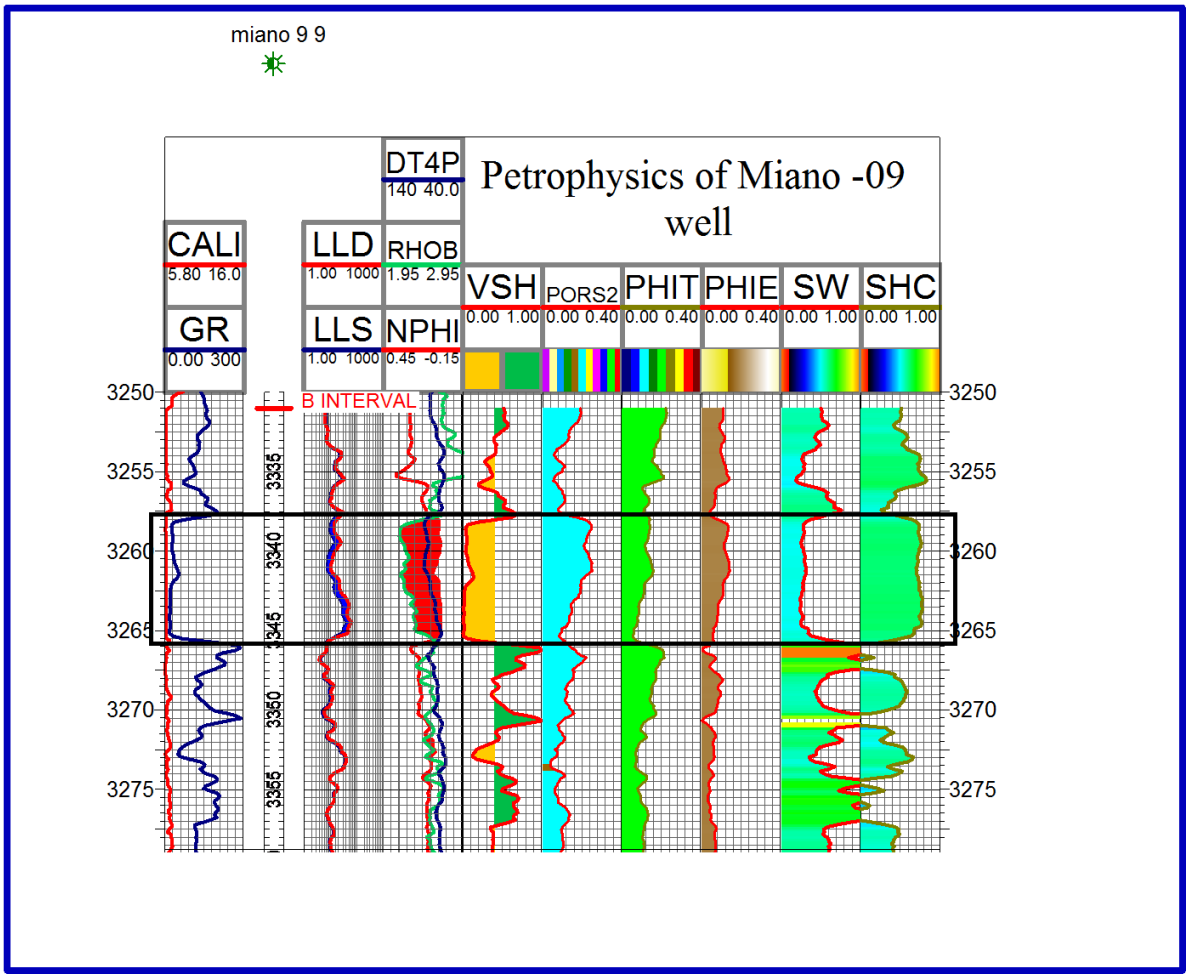

Figure 4.2 Petrophysical analysis of B-sand Miano well-09.

Table 4.2 shows the percentage of different patameters calculated for interested zone and for the entire B-interval zone. The depth of whole B-interval is from 3331m to 3385m, and the interested zone depth is from 3338 to 3346.

Sr #.	Calculation of parameter	Percentage % of entire zone B-interval (3331-3385)m	Percentage % of interested zone (3338-3346)m
1	Average volume of shale (Vsh)	44	24
2	Average porosity (PROS)	11.3	18
3	Average total porosity(PHIT)	11.8	12
4	Average effective porosity (PHIE)	6.4	8
5	Average water saturation (Sw)	51.7	38
6	Average hydrocarbon saturation (Shc)	47.2	62

Table 4.2 calculated parameters for B-interval sand in Miano-09 well.

Chapter 5

Amplitude versus Offset

5.1 Introduction

Technique used to differentiate seismic reflection events caused by lithology changes from those cause by fluid changes is called amplitude versus offset (Crain, 2013). AVO is a technique used by geoscientist to evaluate reservoir's porosity, density, velocity, lithology and fluid content. The energy which is reflected from interface depends on the acoustic impedance and also on the angle of incidence. Because of complexity in the earth subsurface different rock have different AVO response though these rock filled with same fluid and have same porosity **(**Almutlaq and Margrave, 2010).

Individual trace on conventional, (CDP-stacked) Seismic data are assumed to be representative of zero offset (normal incidence) reflection. A vertically incidence p-wave generates only a reflected and transmitted p-wave. The amplitude of reflected wave depends on the reflection coefficient and the amplitude of transmitted wave is dependent on transmission coefficient. In AVO technique the seismic amplitude response of reflection is function of its angle of incidence. Non-zero offset rays when incident at the interface it split into following (knapp et al., 1995).

- Reflected p-wave
- Reflected s-wave
- Transmitted p-wave
- Transmitted s-wave

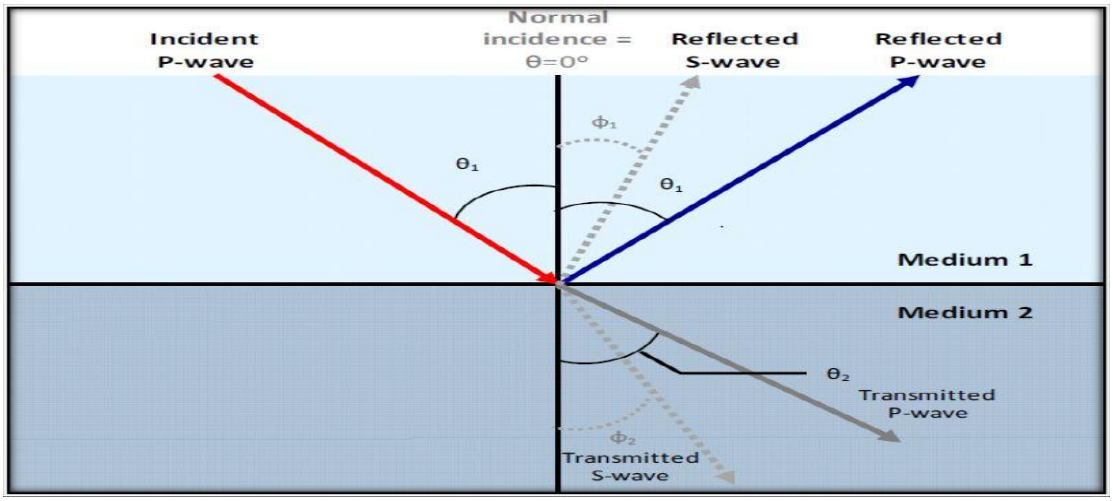

Figure 5.1 Reflection and transmission at the interface for an incident P-wave (Almutlaq & Margrave, 2010).

The amplitude of a reflected p-wave varies with offset according to reflection coefficient, which is dependent on acoustic impedance contrast and Snell's law which is dependent on velocity contrast (Knapp et al., 1995).

5.2 AVO-Modelling

"Bright spots" can be cause by lithologic variations as well as gas sands. Geophysicists in 1980's looked at per stack seismic data and found that amplitude change with offset could be used to explain gas sand capped by shale (Ostrander, 1984). Ostrander also found that there is reduction in poisons ratio related to change in amplitude with offset in the presence of gas.

AVO analysis are done on common-mid point-gathers also known as Ostrander gathers. At each time sample amplitude value from every offset in the gather are curve-fit to a simplified, linear AVO relationship. Schematic flow for process of AVO analysis as shown in Figure 5.2. It shows thee stack section in first step and select the target horizon then in next step there is CDP gathers with different angle of incidence, then in next step there is AVO response of the target horizon which help to understand the class of sand then at the end there is geological interpretation, which help to understand the properties of sand. Then we conclude the percentage of oil and gas in the zone.

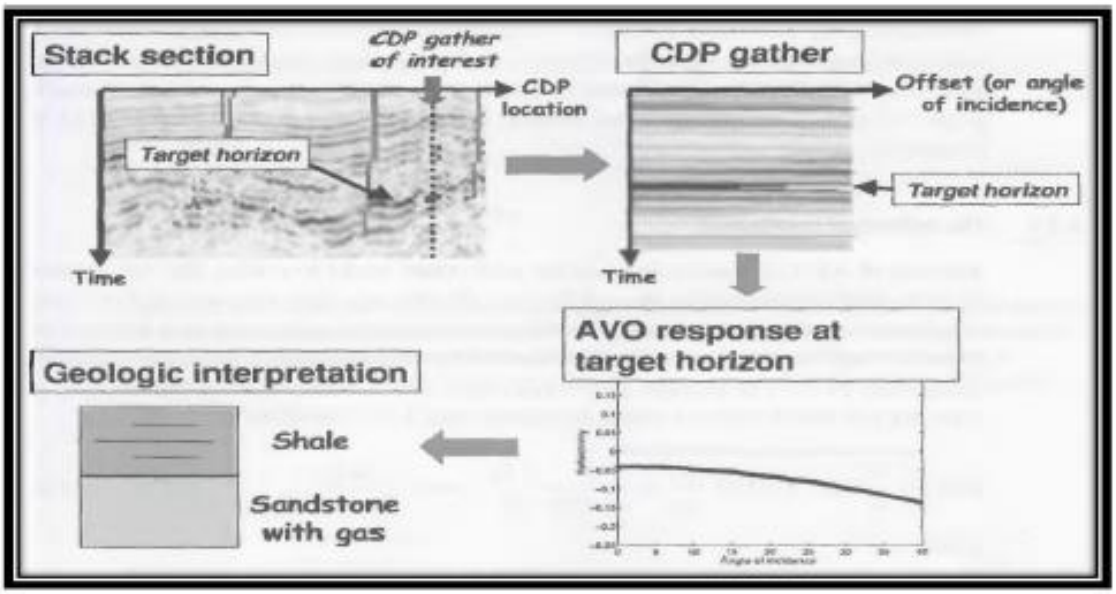

Figure 5.2 Procedure for AVO.

Shuey (1985) confirmed mathematically via approximations to Zoeppritz exact solutions that Poisson's ratio was elastic constant most directly related to offset dependent reflectivity for incident angles upto 40° AVO technology, a commercial tool for oil industry, was born

Conventional AVO (amplitude variation with offset) analysis is based on the well-known Knott and Zoeppritz equations (Knott, 1899, and Zoeppritz, 1919). For a planar interface between two homogeneous isotropic elastic half spaces in welded contact, these equations describe the various reflection and transmission coefficients for plane waves (Treitel and Lines, 1988).

Seismic wave which is reflected at the interface between two media at normal incidence, the expression for the reflection coefficient is given in equation (1).

$$R = \frac{Z_1 - Z_0}{Z_1 + Z_0}, \quad (1)$$

Here R is reflection coefficient, $Z_1$and Z_0 are the acoustic impedance of first and second layers. For non-normal incidence case, in 1919, Karl Bernhard Zoeppritz derived an equation. Three equations are used for AVO modelling.

- Zoeppritz equation
- Shuey's Approximation
- Rouger Approximation

5.3 Zoeppritz equation

The zoeppritz equation gives the exact solution for the division of energy at the reflected and transmitted p-waves and s-waves. Incident energy of wave is divided in to four component which depends upon the p-wave, s-wave velocity, density and incident angle. In 1919, Zoeppritz derive the motion of particle in the reflected and transmitted waves using the conservation of stress and displacement across the interface, which yields four equations with four unknowns.

$$\begin{bmatrix} R_P \\ R_S \\ T_P \\ T_S \end{bmatrix} = \begin{bmatrix} -\sin\theta_1 & -\cos\phi_1 & \sin\theta_2 & \cos\phi_2 \\ \cos\theta_1 & -\sin\phi_1 & \cos\theta_2 & -\sin\phi_2 \\ \sin 2\theta_1 & \frac{V_{P1}}{V_{S1}}\cos 2\phi_1 & \frac{\rho_2 V_{S2}^2 V_{P1}}{\rho_1 V_{S1}^2 V_{P2}}\cos 2\phi_1 & \frac{\rho_2 V_{S2} V_{P1}}{\rho_1 V_{S1}^2}\cos 2\phi_2 \\ -\cos 2\phi_1 & \frac{V_{S1}}{V_{P1}}\sin 2\phi_1 & \frac{\rho_2 V_{P2}}{\rho_1 V_{P1}}\cos 2\phi_2 & \frac{\rho_2 V_{S2}}{\rho_1 V_{P1}}\sin 2\phi_2 \end{bmatrix}^{-1} \begin{bmatrix} \sin\theta_1 \\ \cos\theta_1 \\ \sin 2\theta_1 \\ \cos 2\phi_1 \end{bmatrix} \quad (2)$$

Here equation 2 have four unknown parameters which can be solved, which are;

R_P = Reflected P-wave

R_s = Reflected S-wave

T_p= Transmitted P-wave

T_s= Transmitted S-wave amplitudes

and known values are,

V_{p1}= P-wave velocities for the top layer

V_{s1}= S-wave velocities for the top layer

V_{p2}= P-wave velocities for the bottom layer

V_{s2}= S-wave velocities for the bottom layer

ρ_1= Density for the top layer

ρ_2 = Density for the bottom layer

5.4 Shuey's approximation

In 1985 Shuey simplify the complicated AVO zoeppritz equation (actually, he used the Aki and Richards's approximation to zoeppritz).

Shuey (1985) presented an approximation where the AVO gradient is expressed in terms of the Poisson ration v as follows:

$$R_{pp}(\theta_1) \approx R_{po} + \left[ER_{p0} + \frac{\Delta V}{(1-v)^2}\right] sin^2\theta_1 + \frac{\Delta V_p}{2V_p}(tan^2\theta_1 - sin^2\theta_1) \quad (3)$$

where,

$$R_{po} = \frac{1}{2}\left(\frac{\Delta V_p}{V_p} + \frac{\Delta\rho}{\rho}\right), \quad (4)$$

$$E = F - 2(1+F)\left(\frac{1-2V}{1-V}\right), \quad (5)$$

$$F = \frac{\frac{\Delta V_p}{V_p}}{\frac{\Delta V_p}{\Delta V_p} + \frac{\Delta\rho}{\rho}}, \quad (6)$$

and,

$$\Delta V = V_2 - V_1, \quad (7)$$

$$\mathrm{V} = \frac{(V_2+V_1)}{2}, \quad (8)$$

The coefficients E and F used here in shuey's equation are not the same as those defined earlier in the solution to the zoeppritz equation.

5.5 Ruger's Approximation

Rüger (2001) used the same assumptions of small layer contrast and limited angle of incidence, write the linearized form of SV – to – SV reflection**.**

$$R_{sv-iso}(\theta_s) \approx -\frac{\Delta I_s}{2I_s} + \left(\frac{7\Delta V_s}{2V_2} + 2\frac{\Delta\rho}{\rho}\right) sin^2\theta_s - \frac{\Delta V_s}{2V_2} sin^2\theta_s tan^2\theta_s, \quad (9)$$

5.6 AVO Classification

The most important application of AVO analysis is gas-sand detection. It is noticed that if gas-sand have low VP, VS ratio then we can differentiate it from other lower impedance layers like coals and porous brine sands (Castagna et al., 1993).

Rutherford and Williams in 1989 defined three different classes of gas-sand AVO anomalies which depends upon selected elastic properties of the overburden and reservoir.

When the normal-incidence P-wave reflection coefficient is strongly positive and shows a strong amplitude with decrease in offset and maybe there is change in phase at far offset/angle, it shows the class 1. Its reservoir yields dim spots.

Class 2, for small P-wave reflection coefficients, shows a very large percent change in AVO. In this situation, if the normal-incidence reflection coefficient is slightly positive, a phase change at near or moderate offsets will occur. Class 2 reservoir are difficult to see unless they have appreciable increase of amplitude with offset.

Class 3 anomalies (Rutherford and Williams, 1989) have a large negative normal-incidence reflection coefficient, which becomes more negative as offset increases (these are classical bright spots). A simple rule of thumb that generally applies to shale over gas-sand reflections is that the reflection coefficient becomes more negative with increasing offset (Castagna and Backus, 1993). Class 3 reservoir yield bright spot.

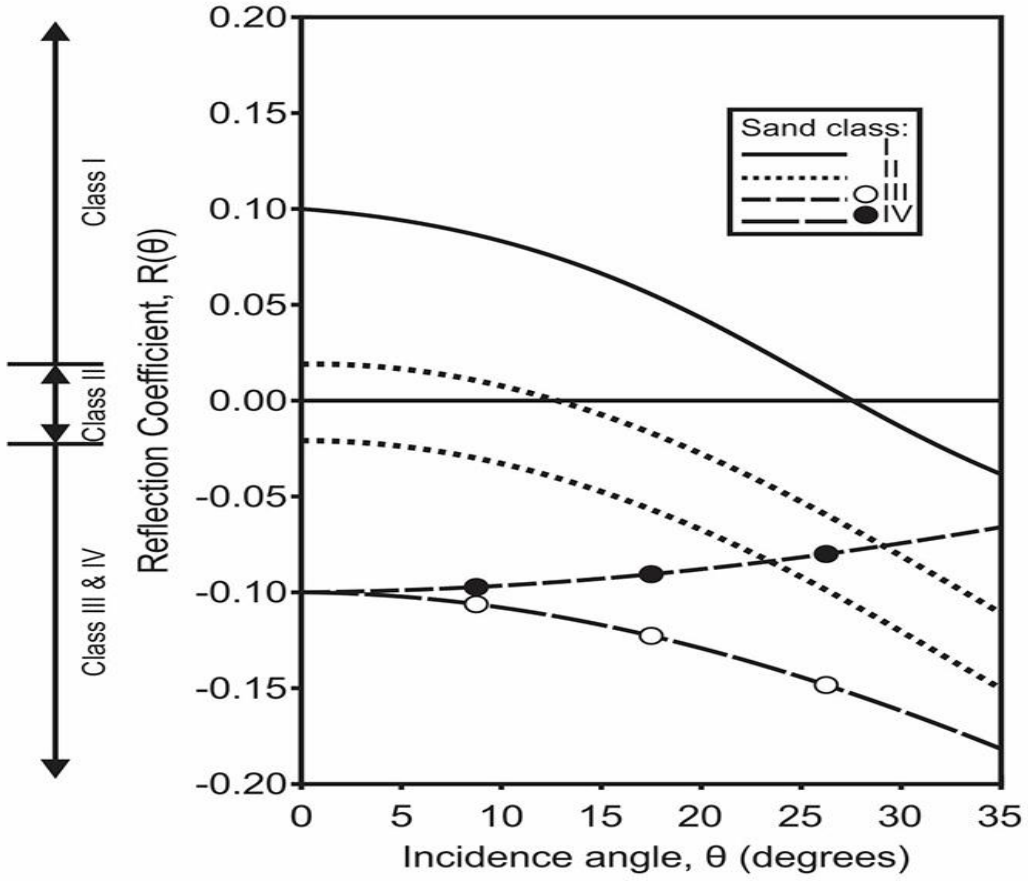

Figure 5.3 AVO classification (Castagna and Swan, 1997).

5.7 AVO modelling for study area

AVO processing should preserve or restore relative trace amplitudes within CMP gathers this implies two goals:

- Correct positioning of reflections in subsurface

- Sufficient data quality that reflection amplitudes have information of reflection coefficients.

However I was provided with well data of the study area Miano, I have data set of Miano-09 well, sonic log is used to calculate the Vp,Vs and density of C-interval and B-interval as mentioned above that B-interval is reservoir rock and C-interval is cap rock. Figure 5.4 shows that exact solution indicates the class one sand behavior in the reservoir zone. So we can say that the reservoir sand is hard as compare to shale present above it. We apply two more approximation in addition to exact solution. We apply these approximation to reduce the complex calculation in the excat solution. The ruger approximation is very close to exact solution for all near, mid and far offset but in shuey approximation the near angles are satisfying exact solution and there is large variation for the mid and far angle with the exact solution. Ruger approximation gives the best results and the shuey approximation. AVO Synthetic display as shown in Figure 5,5, 5.6, 5.7 for Shuey, Ruger and Exact solution. Shuey approximation shows the clearly the polarity reversal for the for offset where as the Exact solution and the Ruger approximation have same polarity.

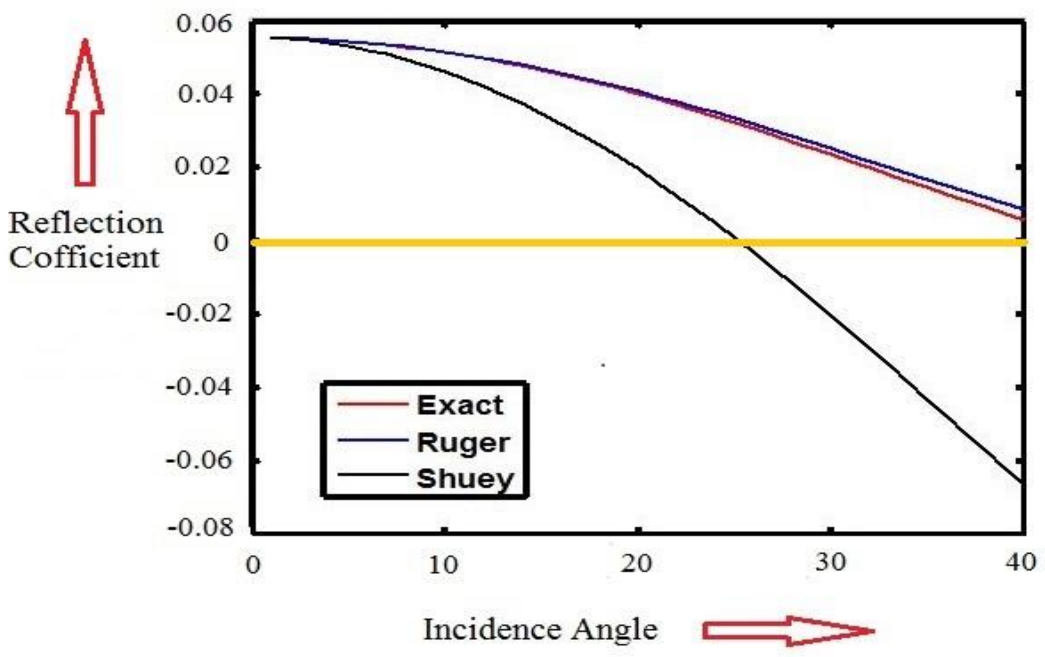

Figure 5.4 AVO plot in study area.

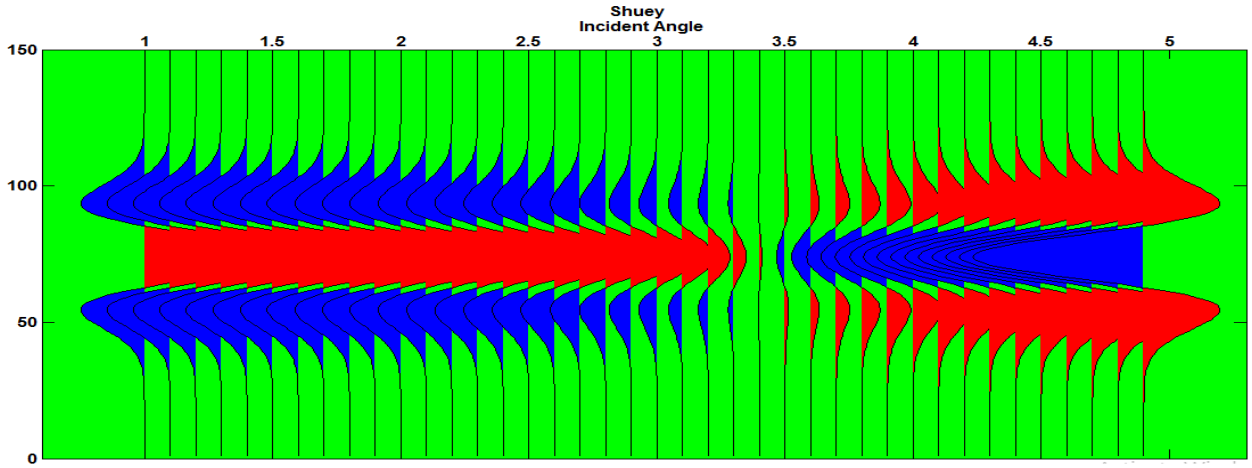

Figure 5.5 AVO synthetic display of Shuey approximation.

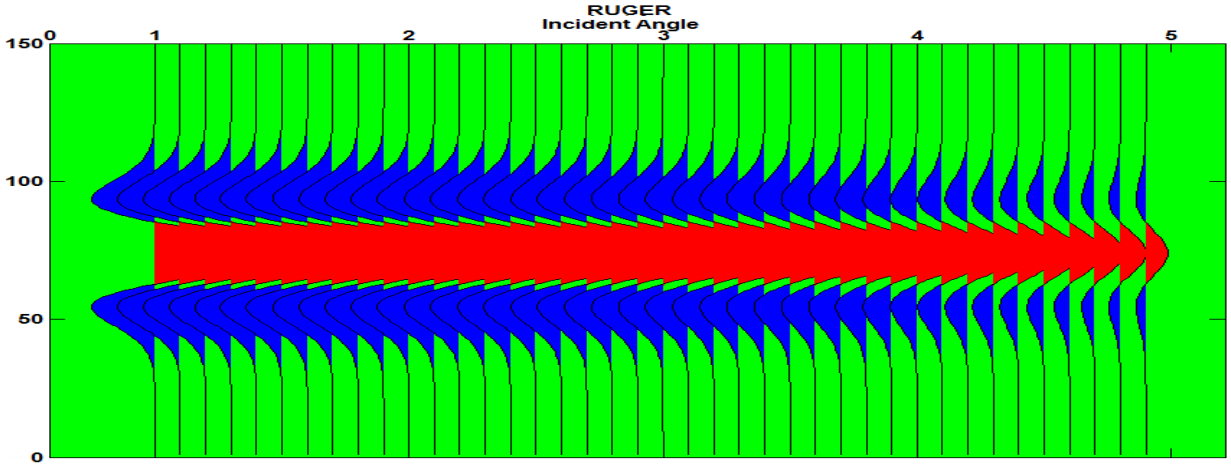

Figure 5.6 AVO synthetic display of Ruger approximation.

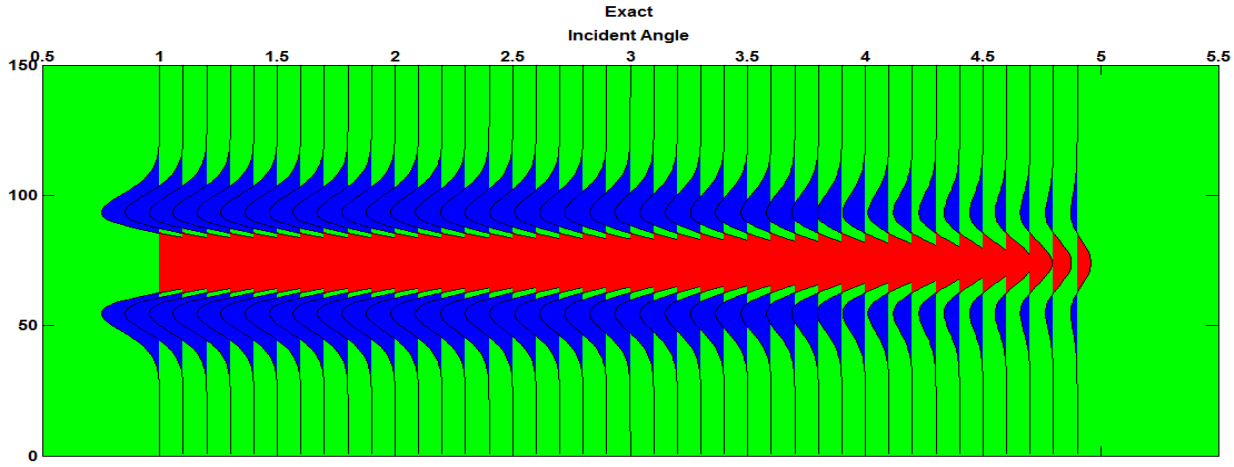

Figure 5.7 AVO synthetic display of exact solution.

Discussion and Conclusion

- From the geology of the area we conclude that the area lies in extensional regim. We conclude from seismic interpretation that there are horst and graben structures in my study area. As the study area lies in the extensional regime which cause normal faulting due to normal faulting horst and graben structure are formed. These horst and graben structure are favorable for accumulation of hydrocarbon. This normal faulting is generated in the results of the Permo Triassic rifting, during the initial Gondwanaland breakup. Subsequent Triassic and Jurassic rifting initiated a marine incursion from the Southeast.
- Complex seismic trace attributes confirm the seismic results but due to seismic data control these attributes did not give best results.
- Petrophysics of Miano-09 well leads to one probable zone for hydrocarbon extraction and the zone of interest lies at depth 3338- 3346 m. In Miano-09 well sand as major lithology was confirmed through GRlog response.
- AVO modelling is performed to check or identify the class and lithology of reservoir zone of the well. AVO modelling for gas-sand identification main lithology of class one sand is confirmed. From AVO plots we confrimed that Zoeppritz and Shuey Approximation shows same polarity for all the angles and Ruger approximation shows polarity reversal for the far angles.

Reference

- Ali, A., Hussain, M., Rehman, K., & Toqeer, M. (2016). Effect of Shale Distribution on Hydrocarbon Sands Integrated with Anisotropic Rock Physics for AVA Modelling: A Case Study. Acta Geophysica, 64(4), 1139-1163.
- Almutlaq, M. H., & Margrave, G. F. Volume 22 (2010). Tutorial: AVO inversion.
- Asquith, G. B., Krygowski, D., & Gibson, C. R. (2004). Basic well log analysis (Vol. 16). Tulsa: American association of petroleum geologists.
- Avseth, P., Mukerji, T., & Mavko, G. (2010). Quantitative seismic interpretation: Applying rock physics tools to reduce interpretation risk. Cambridge university press.
- Badley, M.E, 1985, "Practical Seismic Interpretation", IHRDC publishers, Bostan, 266-70.
- Bell, F. G. (2013). Engineering properties of soils and rocks. Elsevier.
- Burianyk, M., & Pickfort, S. (2000). CSEG Recorder. Canadian Society of Exploration Geophysics.
- Cannon, S. (2015). Petrophysics: a practical guide. John Wiley & Sons.
- Chopra, S., & Marfurt, K. J. (2015). Choice of mother wavelets in CWT spectral decomposition. In SEG Technical Program Expanded Abstracts 2015 (pp. 2957-2961). Society of Exploration Geophysicists.
- Coffeen, J.A., 1986, Seismic Exploration Fundamentals, PennWell Publishing Co.
- Crain, E. R. (2013). Welcome to Crain's Petrophysical Handbook. Online Shareware Petrophysics Training and Reference Manual, url http://www. spec2000. net, Accessed.
- Dewar, J., & Pickford, S. (2001). Rock physics for the rest of us-an informal discussion. CSEG Recorder, 43-49.
- Gibbons, A. D., Whittaker, J. M., & Müller, R. D. (2013). The breakup of East Gondwana: assimilating constraints from Cretaceous ocean basins around India into a best-fit tectonic model. Journal of geophysical research: solid earth, 118(3), 808-822.
- Glover, P.W.J., Geophysical Properties of the Near Surface Earth: Electrical Properties , 11.03, pp. 89-137, in Treatise on Geophysics (2nd Ed.), Ed. G. Schubert, ISBN: 978-0-444-53803-1
- Kadri I.B., (1995), "Petroleum Geology of Pakistan'', PPL, Karachi, Pakistan.
- Kazmi A.H. & Jan M.Q., 1997 "Geology and Tectonic of Pakistan"
- Kearey, P., Brooks, M., & Hill, I. (2013). An introduction to geophysical exploration. John Wiley & Sons.

- Kemal. A. (1991). Geology and new trends for petroleum exploration in Pakistan
- Khan, M. S., Masood, F., Ahmed, Q., Jadoon, I. A. K., & Akram, N. (2017). Structural Interpretation and Petrophysical Analysis for Reservoir Sand of Lower Goru, Miano Area, Central Indus Basin, Pakistan. International Journal of Geosciences, 8(04), 379.
- Knapp, R. W., Hedke, D. E., & Anderson, N. L. (1995). Amplitude Variation with Offset. BULLETIN-KANSAS GEOLOGICAL SURVEY, 34-38.
- Koson, S., Chenrai, P., & Choowong, M. (2014). Seismic Attributes and Their Applications in Seismic Geomorphology. Bulletin of Earth Sciences of Thailand, 6(1), 1-9.
- Krois P, Mahmood T and Milan G., 1998, Miano Field, Pakistan, a case history of model driven exploration, Pakistan Petroleum Convention, November 1998, Islamabad.
- Lines, L. R., & Newrick, R. T. (2004). Fundamentals of geophysical interpretation. Society of Exploration Geophysicists.
- Lines, L. R., Schultz, A. K., & Treitel, S. (1988). Cooperative inversion of geophysical data. *Geophysics*, *53*(1), 8-20.
- Majid, K., Shahid, N., Munawar, S., & Muhammad, H. (2016). Interpreting Seismic Profiles in terms of Structure and Stratigraphy with Implications for Hydrocarbons Accumulation, an Example from Lower Indus Basin Pakistan. J Geol Geophys, 5(257), 2.
- McQuillin, R., Bacon, M., and Barcaly, W., 1984 An introduction to seismic interpretation, Graham & Trotman Limited Sterling House, 66 Wilton Road London SW1V 1DE
- Nissen, S. E. (2002). Seismic attributes for the explorationist. Kansas Geological Survey, Open-file Report, 49, 34-35.
- Oil and gas fields are geological features that result from the; source rocks, Migration, reservoir rocks, seals, and traps (Sroor, 2010).
- Onajite, E. (2013). Seismic data analysis techniques in hydrocarbon exploration. Elsevier.
- Osuoji, O. U., Alile, O. M., Airen, J. O., Ikonmwen, M. O., & Isichei, B. (2013). Construction and Interpretation of Structural Map Using Seismic Reflection Times in Location of Prospective Hydrocarbon Trap. Science and Technology, 3(4), 127-135.
- Oyeyemi, K. D., & Aizebeokhai, A. P. (2015). Seismic attributes analysis for reservoir characterization; offshore Niger Delta. Petroleum and coal, 57(6), 619-628.
- Powell, C. AcA., 1979. A speculative tectonic history of Pakistan and sorroundings: some constraints from the Indian Ocean. In: A. Farah and K.A Dejong (Editors), Geodynamics of Pakistan. Geol. Surv.Pak., Quetta.

- Rehman, K., Manawer, M., & Ahmed, S. (2013). Delineation of seismic reflectors in Miano area. Journal of Himalayan Earth Sciences, 46(2), 25-34.
- Rutherford, S. R., & Williams, R. H. (1989). Amplitude-versus-offset variations in gas sands. Geophysics, 54(6), 680-688.
- Sheriff R. E., Telford W. M., and Geldart L. P., 1990, Applied geophysics, Cambridge University Press.
- Sroor, M. (2010). Geology and Geophysics in Oil Exploration. Mahmoud Ahmed Sroor.
- Steve, M. (1955). U.S. Patent No. 2,719,038. Washington, DC: U.S. Patent and Trademark Office.
- Subrahmanyam, D., & Rao, P. H. (2008). Seismic attributes–A review. In 7th International Conference and Exposition on Petroleum Geophysics, Hyderabad, India.
- Taner, M. T. (2000). Attributes Revisited. Technical Publication, Rock Solid Images, Inc, Houston, Texas
- Taner, M. T., Schuelke, J. S., O'Doherty, R., & Baysal, E. (1994). Seismic attributes revisited. In SEG Technical Program Expanded Abstracts 1994 (pp. 1104-1106). Society of Exploration Geophysicists.
- Taner, M.T., Koehler,F. and Sheriff, R.E., 1979, Complex Seismic Trace analysis, Geophysics, Vol. 44(6), pp.1041-1063
- Tittman, J., & Wahl, J. S. (1965). The physical foundations of formation density logging (gamma-gamma). Geophysics, 30(2), 284-294.
- Wandrey, C. J., Law, B. E., & Shah, H. A. (2004). Sembar Goru/Ghazij composite total petroleum system, Indus and Sulaiman-Kirthar geologic provinces, Pakistan and India. US Department of the Interior, US Geological Survey.
- Zoeppritz, K., 1919, Erdbebenwellen VIIIB, On the reflection and propagation of seismic waves: Göttinger Nachrichten, I, 66-84.